COMPOSITE STRUCTURAL PROGRAM

RENSSELAER POLYTECHNIC INSTITUTE TROY, N.Y. 12181

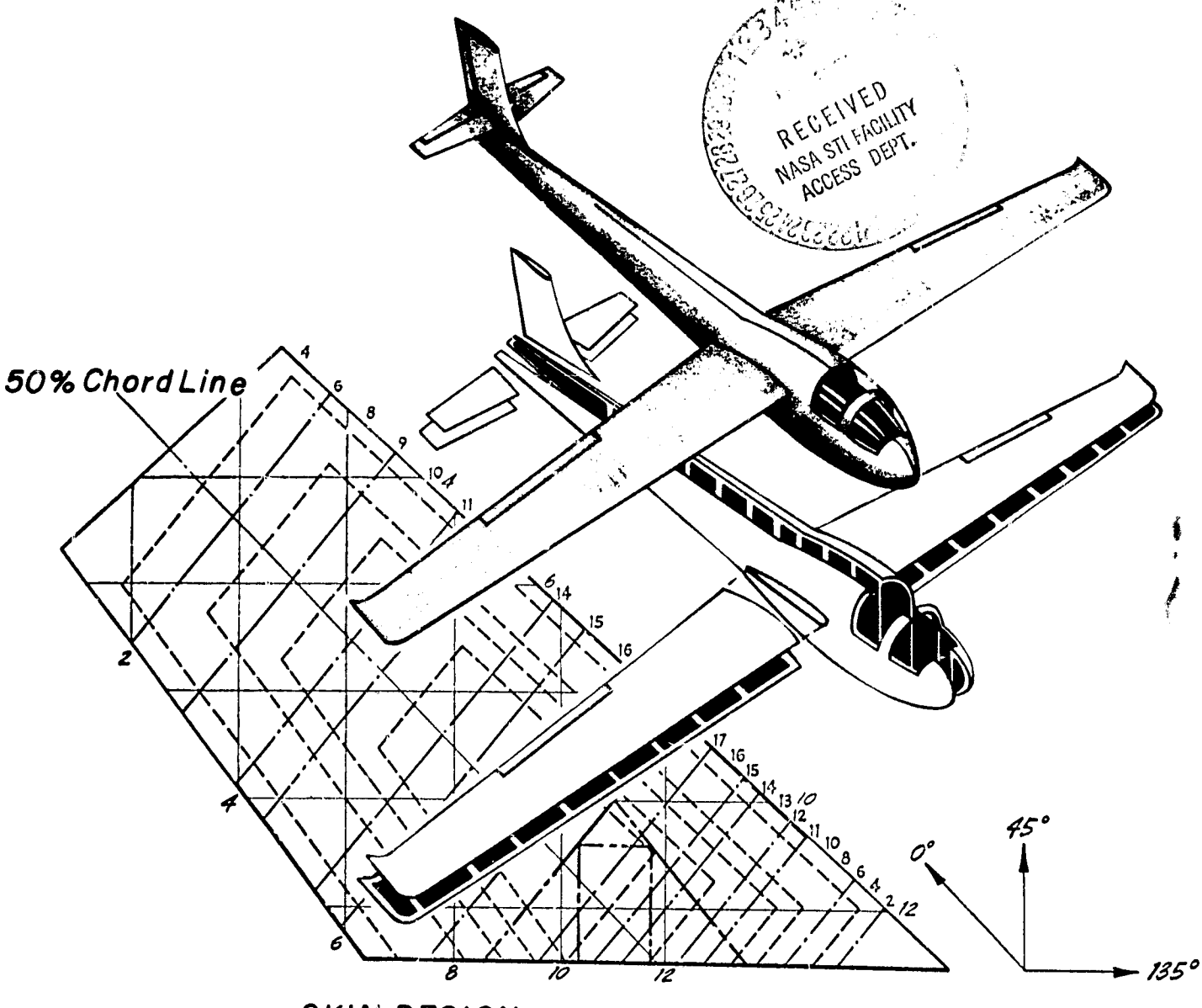

SKIN DESIGN

(NASA-CR-162578) COMPOSITE STRUCTURAL MATERIALS Semiannual Report, Apr. - Sep. 1979 (Rensselaer Polytechnic Inst., Troy, N. Y.) 107 p HC A06/MF A01 CSCL 01C

N80-15076

Unclas
G3/05 46699

SPONSORED BY NASA/AFOSR

Semi-Annual Progress Report

April 1979 - September 1979

COMPOSITE STRUCTURAL MATERIALS

Air Force Office of Scientific Research
and
National Aeronautics and Space Administration
Grant No. NGL 33-018-003

Co-Principal Investigators:

George S. Ansell
Dean, School of Engineering

Robert G. Loewy
Institute Professor

and

Stephen E. Wiberley
Dean, Graduate School and Vice Provost

Rensselaer Polytechnic Institute
Troy, New York 12181

NASA Technical Officer

Leonard A. Harris
Materials and Structures Division
NASA Headquarters

CONTENTS

INTRODUCTION

The longstanding technological demand for improved performance in materials continues unabated. In fact, the promise of more than a decade in filamentary composite materials has generated intense interest. Such interest is well founded, having been generated by the possibility of using brittle materials with high modulus, high strength, but low density in composites which fail in a non-catastrophic manner. Such fiber reinforced composite materials offer substantially improved performance and potentially lower costs for aerospace hardware.

Fulfilling the promise of composite materials, however, requires a strong technology base. NASA and AFOSR have realized that to fully exploit composites in sophisticated aerospace structures the technology base must be improved. This, in turn, calls for expanding fundamental knowledge and the means by which it can be successfully applied in design and manufacture. It also calls for expanding the body of engineers and scientists competent in these areas. As part of their approach to accomplishing this, NASA and AFOSR have funded the current composites program at Rensselaer. The purpose of the RPI composites program is to develop advanced technology in the areas of physical properties, structural concepts and analysis, manufacturing, reliability and life prediction. Concommitant goals are

to educate engineers to design and use composite materials as normal or conventional materials. A multifaceted program has been instituted to achieve these objectives. The major elements of the program are:

1. CAPCOMP (Composite Aircraft Program Component). CAPCOMP is primarily a graduate level project being conducted in parallel with a composite structures program sponsored by NASA and performed by a private, aerospace manufacturing contractor. The first component redesign is being done in conjunction with the Boeing Commercial Airplane Company. The main spar/rib region on the Boeing 727 elevator, near its actuator attachment point, has been selected, with Boeing's advice and the concurrence of NASA/AFOSR, for study in CAPCOMP. The magnitude of the project - studying, designing, fabricating and testing a relatively small but highly stressed region on the elevator - is both consistent with Rensselaer's capabilities and a significant challenge. The selection of a portion of a full-scale flight hardware structure assures relevance to this project's direction.

Visits to Boeing were conducted in the Fall of 1978 by Professor Hoff and several of his students, and the first serious design work began shortly thereafter. Two alternative designs were pursued to the point of preliminary analysis and testing; further progress is reported in Part I.

2. CAPGLIDE (Composite Aircraft Program Glider). This undergraduate demonstration project is to design, fabricate and test a foot-launched, ultralight glider using composite structures. A flight vehicle was selected to maximize student interest and to provide the students with a broad-based engineering experience. For those students continuing with graduate work at RPI, CAPGLIDE is intended to provide natural progression to CAPCOMP. The progress on the CAPGLIDE project to date has been very good. Seven professors and approximately 30 students were actively engaged in the project during the beginning of this period; that is, at the end of the spring semester. A description of the status of the work performed under CAPGLIDE to the end of this reporting period is given in Part II.

3. COMPAD (Computer Aided Design). A major thrust of the composites program is to develop effective and efficient tools for the analysis and design of composite structures. Rensselaer and NASA Langley have jointly implemented the use of the SPAR code on minicomputers, and the work at Rensselaer has made "virtual memory" available to those using SPAR. Recently attention has turned to preprocessor developments; details are reported in Part III.

4. Composites Fabrication and Test Facility. Structural design engineers, educated only by course work and design projects limited to paper, often fail to sense or appreciate problems involved in fabrication. The actual

fabrication and testing of composite structural components provides this training and the final validation for the designs in our CAP projects. RPI's Composites Fabrication and Test Facility is located in the laboratory and high bay areas of the Jonsson Engineering Center. Equipment is available for compression molding parts as large as 19" x 19" and vacuum bagging parts of much larger size. Panels approximately 4' x 20' have been made by vacuum bagging. Specifics are given in Part II, CAPGLIDE. A pressure vessel for small parts and spars has been designed and built. A second one capable of higher pressures is also planned; more complete details are reported in Part I, CAPCOMP.

Our capabilities and efficiency in fabrication and testing were increased substantially during the reporting period by the addition of a Manager and Master Technician for the Composites Laboratory. This position is filled by Volker Paedelt whose background includes almost twenty years at the Vereinigte Deutsche Metallwerke, Frankfurt, Germany; Simmons Fastener, Menands, N. Y. and the Physics Department at Rensselaer Polytechnic Institute

5. INSURE (Innovative and Supporting Research). The criteria for selection of research projects to be conducted under this program are (a) that they must anticipate critical problem areas which may occur in the CAP or NASA/AFOSR programs or (b) that solutions to existing problems are not yet satisfactorily in hand. During the reporting period

five programs were funded. Results from the ongoing projects are reported in Part IV.

6. Curriculum Revisions. The goal of educating engineers to think of composites as normal or conventional materials has required changes in curriculum. Since the initiation of this program, almost all Rensselaer engineers take introductory courses which incorporate the concepts of anisotropy and composite materials. In addition, six specialized courses in composites have been offered during the past three years to develop those special skills required of students involved in the composites program. A new course was introduced in the Fall of '78 semester on composite design and analysis using programmable hand calculators, a central mini and full frame computers. A new graduate level advanced topics course with the title "Advanced Finite Elements" was offered for the first time in September 1979.

The additions of the SAP and SPAR computer codes and the growing availability of interactive computer graphics under our COMPAD program element have reached the point where our engineering students are using these facilities as everyday working tools for design, analysis and visualization purposes. We have thus achieved one of the principal goals of the curriculum development activities.

7. Technical Interchange.

a) Dr. Kiyoshi Kenmochi returned to the Industrial Products Research Institute of Japan's Industrial Science & Technology

Agency in August. He was most helpful during his appointment as Research Associate under the program, having set up our photoelastic stress analysis facilities and assisting us in conducting the mechanical attachment research reported in our last report (July, 1979) and herein.

b) Technical Meetings: Technical meetings, on- and off-campus, provide important opportunities for interchange of technical information. Because of the large number of composites meetings, a central catalog with all upcoming meetings is being maintained and distributed periodically. In this way we help assure that a Rensselaer staff member will participate in important meetings. The calendar for this reporting period is shown in Table I. Meetings attended by RPI composites program faculty/staff during the reporting period are shown in Table II. Some meetings particularly relevant to composites, held on-campus with off-campus speakers, are listed in Table III. A list of composite-related visits to relevant organizations by RPI faculty/staff/students, with the purpose of each visit outlined, is presented in Table IV. Regular readers of these progress reports will note the higher level of such activity in the months from September to April - partially because full academic year programs are in session - than in those reports covering periods including the summer.

In summary, the NASA/AFOSR Composites Aircraft Program is a multi-faceted program whereby aeronautical, mechanical

TABLE I
CALENDAR OF COMPOSITES-RELATED MEETINGS
for the period April '79 to September '79

1979

4/4-6	20th Structures, Structural Dynamics & Materials Conf., St. Louis, Mo. Sponsored by AIAA/ASME/ASCE.
4/16-27	Very Large Vehicle Conference, Arlington, Va. Sponsored by AIAA.
5/7-10	Design Engineering Conference & Show, Chicago, Ill. Sponsored by ASME.
5/9-11	Materials Conference, Washington, D. C. Sponsored by ASME.
5/14-17	Conference on Space Manufacturing Facilities, Princeton, N. J. Sponsored by Princeton and AIAA.
5/21-25	Fracture of Composites, San Francisco, Ca. Sponsored by Society for Experimental Stress Analysis.
5/21-25	High Modulus Fibers & Their Composites, San Francisco, Ca. Sponsored by ASTM.
5/22-23	Symposium on the Fatigue of Composite Materials, San Francisco, Ca. Sponsored by ASTM.
5/23-25	Advanced Composites: Design and Applications, Gaithersburg, Md. Sponsored by National Bureau of Standards, NASA and NADC.
6/14-16	Reinforced Plastics/Composites, Chicago, Ill. Sponsored by Plastics Seminars.
6/18-20	Applied Mechanics, Fluids Eng. and Bioeng. Conference, Niagara Falls, N. Y. Sponsored by ASME and CSME.
6/25-29	Pressure Vessels & Piping Conference, San Francisco, Ca. Sponsored by ASME.
6/25-29	Conference on Carbon, University Park, Pa.
7/11-13	Lighter-than-Air Systems Technology Conference, Palo Alto, Ca. Sponsored by AIAA.
8/6-10	Sixth Annual Conference on Computer Graphics & Interactive Techniques, Chicago, Ill.
8/20-22	Aircraft Systems & Technical Meeting, New York, N. Y. Sponsored by AIAA.
9/3-7	Practical Applications and Design of Fibre Composites, University of Cambridge, England.
9/10-12	Design Engineering Technical Conference, St. Louis, Mo. Sponsored by ASME.
9/10-13	International Conference on Acoustic Emission, Anaheim, Ca. Sponsored by ASNT.
9/11-14	International Forum: Composites, Assemblage & Adhesion, Lyon, France.

TABLE II
COMPOSITES-RELATED TECHNICAL MEETINGS ATTENDED OFF-CAMPUS
for the period April '79 to September '79

1979

5/21-26 ASTM Symposium on Composite Materials, Visit EPRI and Lawrence Livermore Lab. (Prof. Stoloff).

5/21-22 American Helicopter Society Forum (Prof. Loewy), Washington, D. C.

5/21-24 ASTM Fatigue Conference on Composites (Prof. Krempl), San Francisco, California.

6/7-8 Conference at National Bureau of Standards on Technical Cooperative Center for Composites (Prof. LeMaistre), Washington, D. C.

7/11-13 Acoustical Society of America Meeting, (Prof. Das and C. Lanzl), Boston, Massachusetts.

TABLE III
COMPOSITES-RELATED MEETINGS/TALKS HELD AT RPI
(April '79 - September '79)

Topic	Date	Speaker(s)
Finite Element Analysis of the Post Buckling Behavior of Curved, Laminated, Composite Panels	4/9/79	N. J. Kudva, Virginia Polytechnic Inst.
Structural Design for Longivity: A Professor's View	4/24/79	James W. Mar, Massachusetts Institute of Technology
Stress Analysis Around Macroscopic Cracks Under Creep Conditions	4/27/79	Hermann Reidel, Max Planck Institute for Iron Study
The Effect of Statistical Correlation on Weakest Link Systems	5/3/79	R. C. Garson, University of Pittsburgh
Aromatic Polyamides: Development and Uses	10/10/79	Paul W. Morgan, formerly Research Associate, E. I. duPont de Nemours and Co.
New Methods in High Temperature Structural Design	10/11/79	Donald Griffin, Westinghouse Corporation
World Trends in Computer-Aided Manufacturing	10/25/79	M. Eugene Merchant, Director of Research Planning, Cincinnati Milacron, Inc.

TABLE IV

COMPOSITE-RELATED VISITS TO RELEVANT ORGANIZATIONS

by RPI Faculty/Staff/Students

Visited	Date	by Prof(s)	Purpose
AFOSR: Dr. L. Kravitz, Director	5/10/79	R. Loewy	To discuss NDE, Fatigue and Failure Mechanisms
W.P.A.F.B.: Mr. G. Peterson and personnel of AFML and AFFDL	7/30/79	J. Diefendorf L. Feeser G. Helwig R. Loewy S. Sternstein	To discuss the NASA/AFOSR Program and USAFML amd USAFFDL programs in composites

and materials engineers must interact to achieve its goals. "Hard-nosed" engineering of composite aircraft structures is balanced against research aimed at solving present and future problems. In the following sections, detailed descriptions of the CAPCOMP, CAPGLIDE, COMPAD and INSURE programs are presented.

PART I

CAPCOMP (Composite Aircraft Program Component)

CAPCOMP (Composite Aircraft Program Component)
(N. Hoff, R. Loewy)

CAPCOMP is a program to design flight critical structures to take the maximum advantage of composite materials. By combining the efforts of experienced faculty with bright and well trained but inexperienced graduate students in an environment relatively free of traditional design and manufacturing processes, we hope to devise new and hopefully useful design concepts.

There is sufficient information available today to prove that many structural elements can be built lighter of advanced composites than of metals. But if such elements have to be joined by any other method than adhesive bonding, difficulties and uncertainties arise which can be eliminated only through conservative designs with their attendant penalties in weight or by extensive and expensive programs of "cut and try". This stands as one important impediment to full adoption of composites by the aerospace industry.

On the basis of these considerations Rensselaer Polytechnic Institute began, as the first task aimed at new structural concepts, the design using composites of a joint used in an airplane elevator. To make the design realistic, an existing metal airframe component was chosen for redesign in composites. The existing design chosen was that of the Boeing 727 elevator actuator attachment. We conceive of this work as carrying forward a Structures Demonstration

Program using the joint of the 727 elevator, paralleling that of NASA and its aerospace engineering contractor, the Boeing Commercial Airplane Company. Our design, fabrication and test effort will emphasize design ideas specifically suited to advanced composite construction for the purpose of minimizing the weight of the structure, but on a scale consistent with the university context and funding level. The staff of RPI is very grateful to the Boeing Company and its engineers for their wholehearted support of the work at RPI.

During the reporting period, the two different designs reported previously (July, 1979) as suitable for replacing the largely metal attachment produced by Boeing were pursued. The first, using quasi-isotropic graphite-epoxy laminates (the R. W. Berg design), was chosen for initial fabrication and second-round stress analysis. The second (C. Muser) design, in which a deliberate attempt was made to use uniaxial graphite-epoxy tape to as great an extent as possible, was suspended in favor of new design analyses and test planning with the objective of optimizing the strength of the movable, heavily loaded bolted joint attachment point.

The research aimed at maximizing the load carrying ability of the attachment of the rib flanges to the elevator skin through mechanical (i.e., pin-type) fasteners also continued. The literature and theory of empty and loaded

circular holes in composite plates was reviewed as part of the process of determining the most efficient arrangement of fibers around the hole.

These efforts have been jointly directed by Dr. Nicholas J. Hoff, in part-time arrangement, and by Dr. Robert G. Loewy. They are described further in the following paragraphs.

1. The Elevator and Its Attachment

The conventional aluminum alloy elevator of the Boeing 727 is shown in the upper half of Figure 1. The lower half of the figure is the new version of the elevator redesigned by Boeing in graphite epoxy; it is evident from the pictures that the latter is composed of fewer parts than the former. However, the actuator fitting of the new design is still manufactured of aluminum alloy. This fitting is shown in Figure 2. The fitting is attached to outboard and inboard portions of a new graphite-epoxy spar and to a graphite-epoxy nomex-honeycomb rib as indicated in Figure 3.

The attachment was designed by Boeing to carry loads up to 19,000 lbs. The direction of the load varies as the elevator rotates over an angle of 28 degrees from the full-down to the full-up position.

2. Berg's Design

Berg's design is shown in Figures 4 and 5. The first

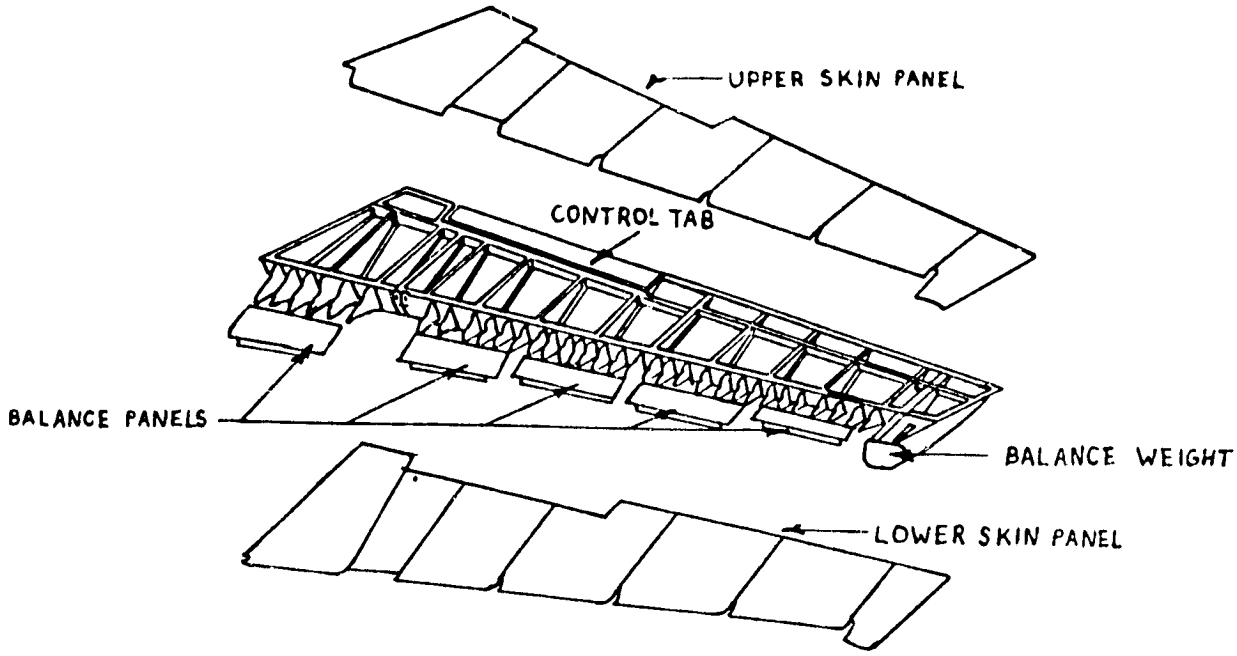

Conventional Aluminum Elevator

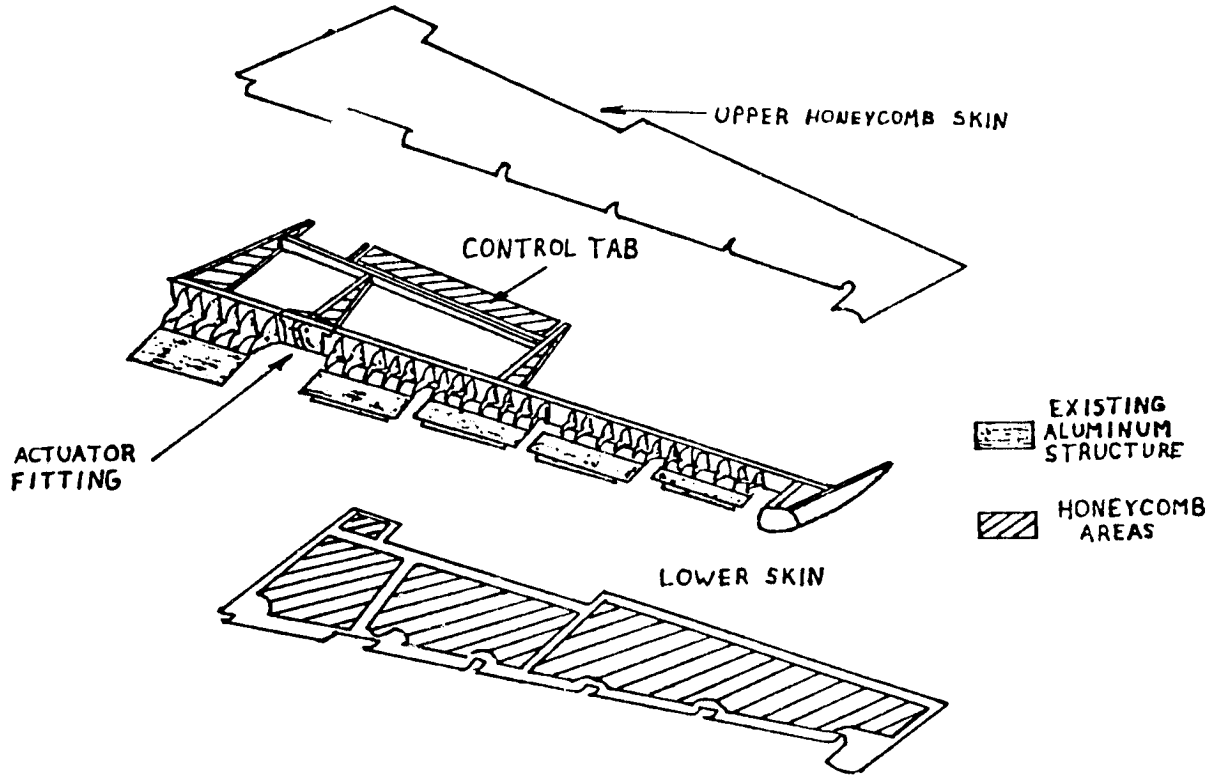

Advanced Composite Elevator

BOEING ELEVATOR ASSEMBLY

Figure 1

ALUMINUM ACTUATOR FITTING (Boeing Design)

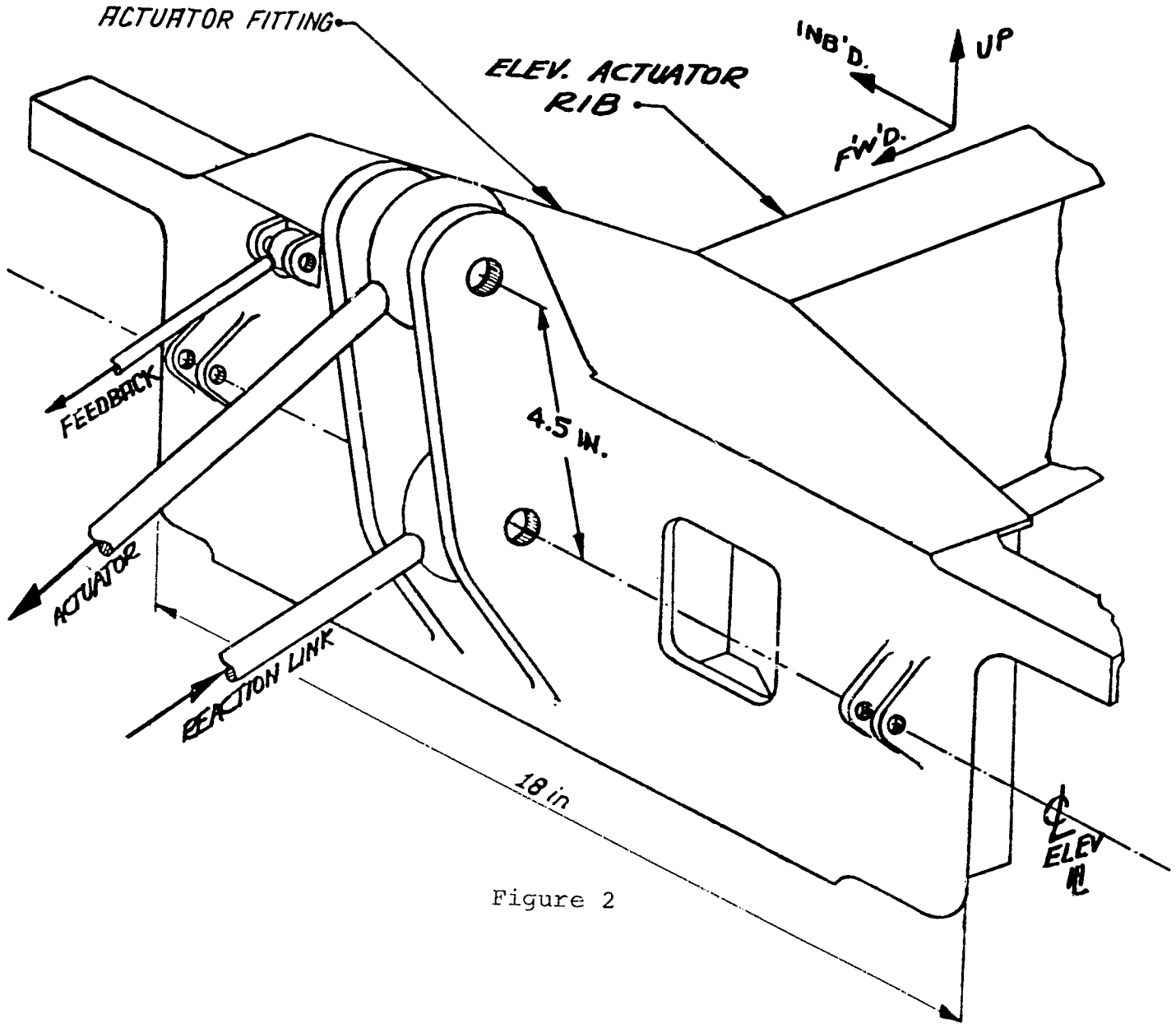

Figure 2

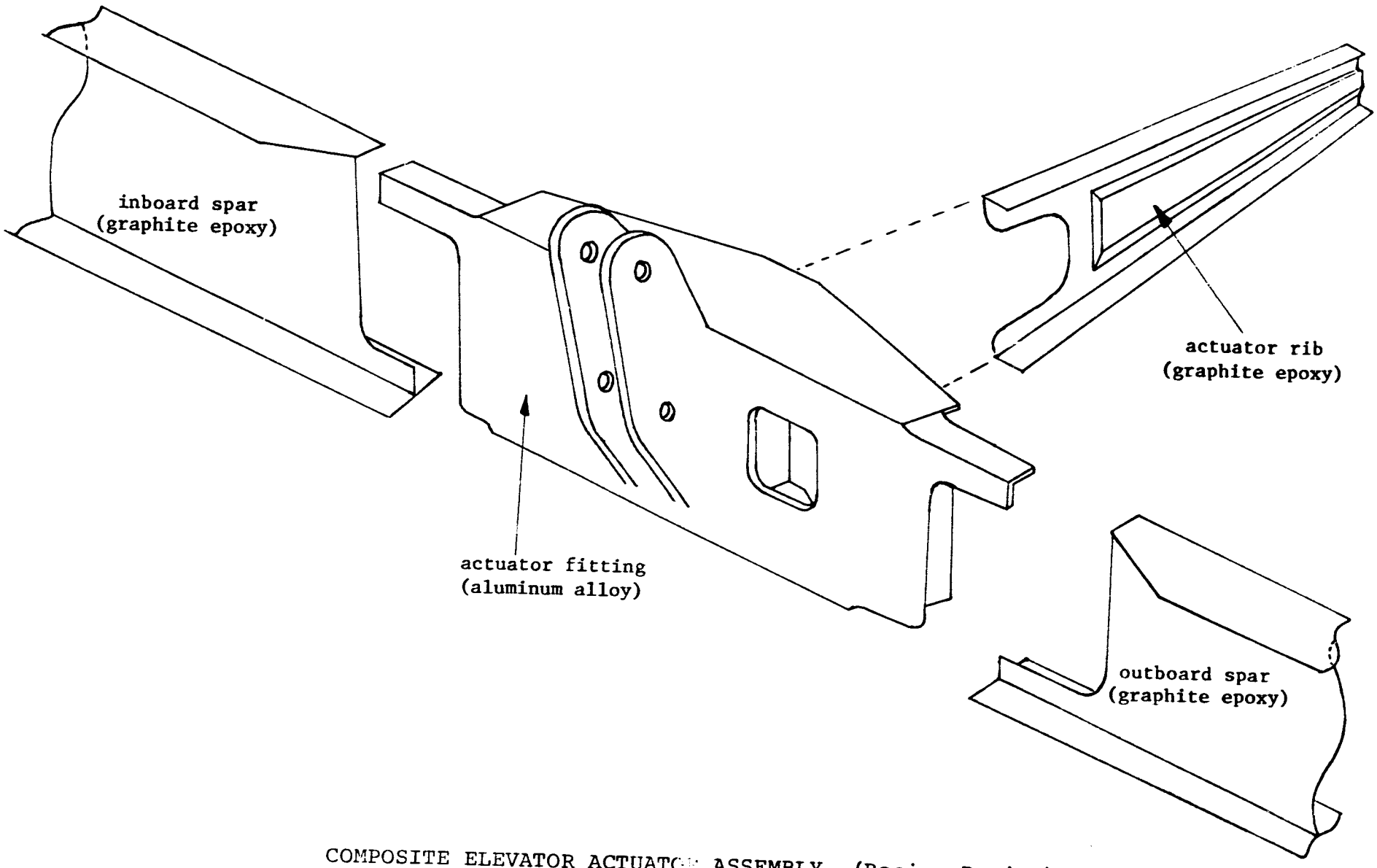

COMPOSITE ELEVATOR ACTUATOR ASSEMBLY (Boeing Design)

Figure 3

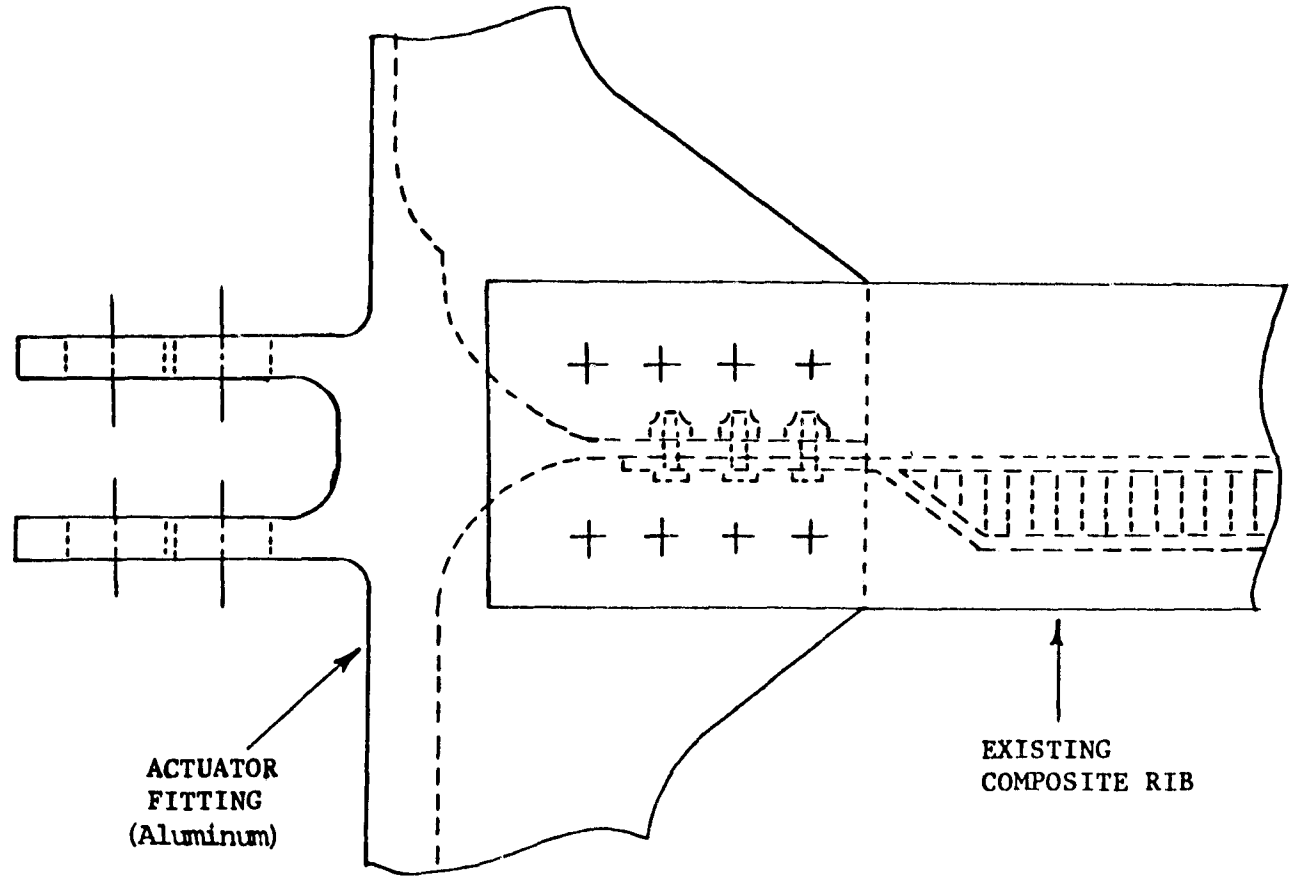

PRESENT DESIGN

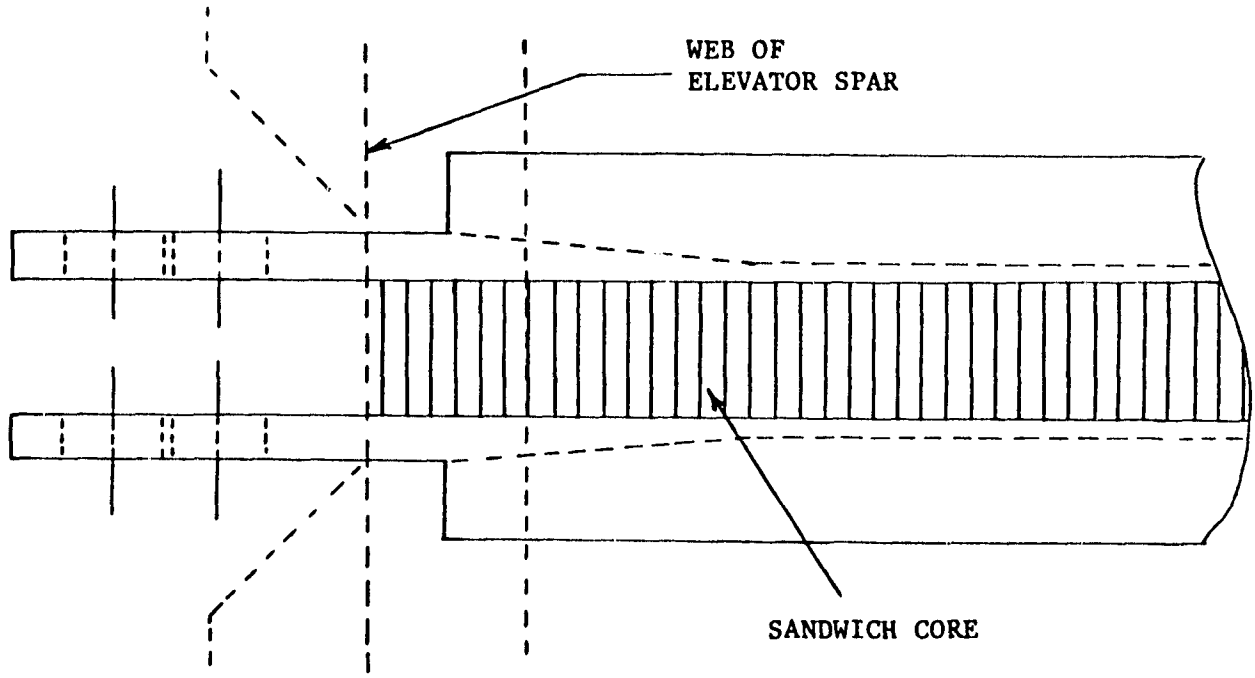

PROPOSED DESIGN (Berg)

ACTUATOR LUG TO RIB TRANSITION - TOP VIEW

Figure 4

PROPOSED SPAR AND RIB ASSEMBLY (Berg Design)

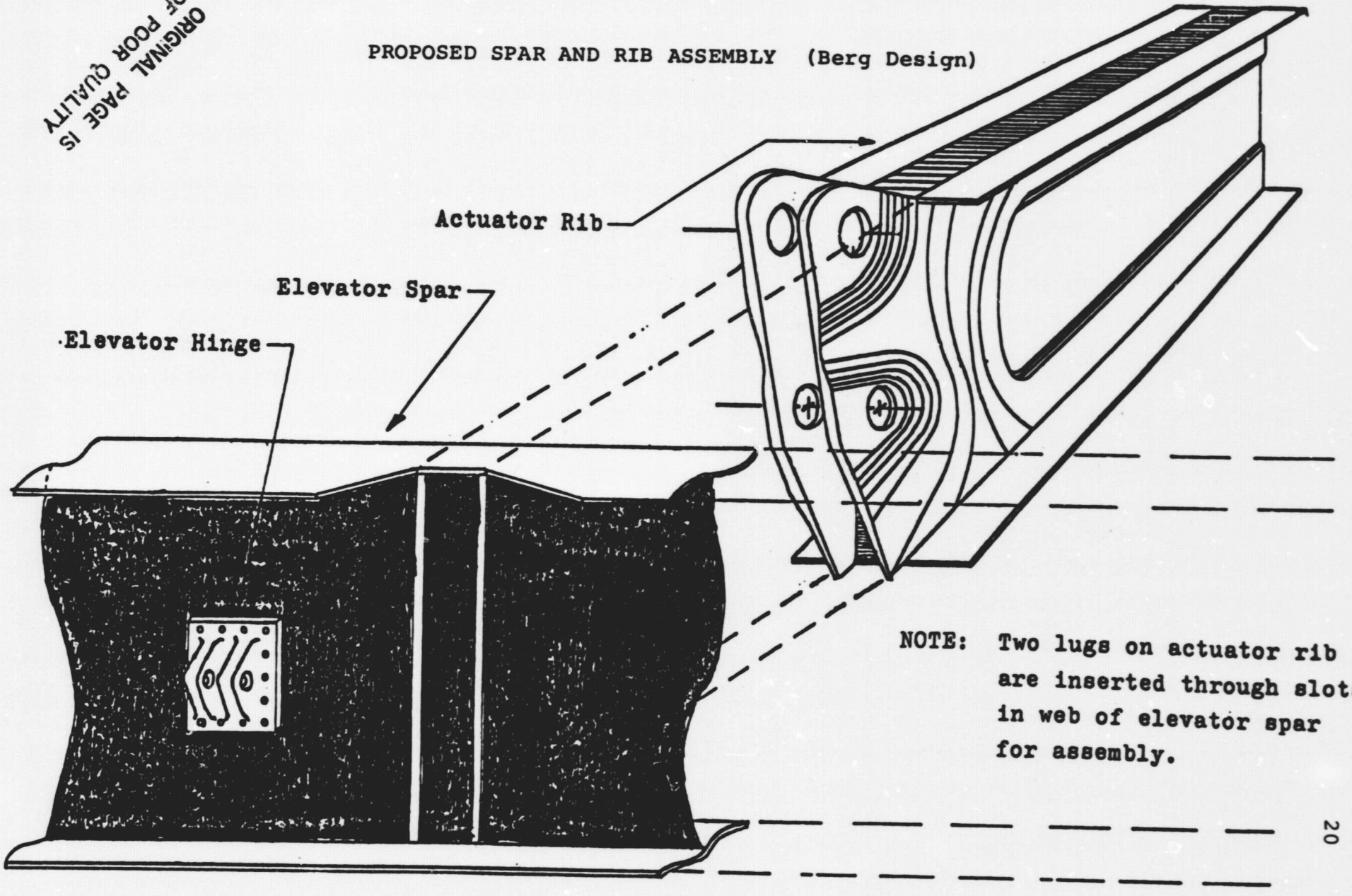

NOTE: Two lugs on actuator rib are inserted through slots in web of elevator spar for assembly.

Figure 5

of these figures compares the Boeing composite design with Berg's design; both are shown. Figure 5 shows how the spar and new actuator rib would be assembled and the build-up of thickness in the lug areas anticipated, as needed, to provide the required bearing strength. Note that the edges of some of the layers are bent 90 degrees to form flanges to which the upper and lower coverplates of the elevator can be attached. Attachment would be by means of titanium Hi-Loc fasteners. The right-hand and left-hand graphite-epoxy webs are stabilized by a layer of nomex-honeycomb between them.

The finite-element analysis of the actuator rib web (including the areas of the lugs with the bolt holes) reported for the last period has been refined. In the first computation, the wall thickness of the actuator rib web was taken as constant to examine the stress distribution in the area of the holes and the way these stresses transfer loads to the flanges of the actuator rib. The mathematical model contained 482 nodes and a total of 800 quadrilateral and triangular elements (see Figure 6), introduced forces simulating bolt loads from the actuator and reaction links (see Figure 2) and a distributed shear flow along the upper and lower edges of the actuator rib to represent the reacting torque resulting from aerodynamic forces on the elevator.

In the current reporting period the analysis was repeated for a variable thickness web, using the same mathematical models. Several iterations were made examining

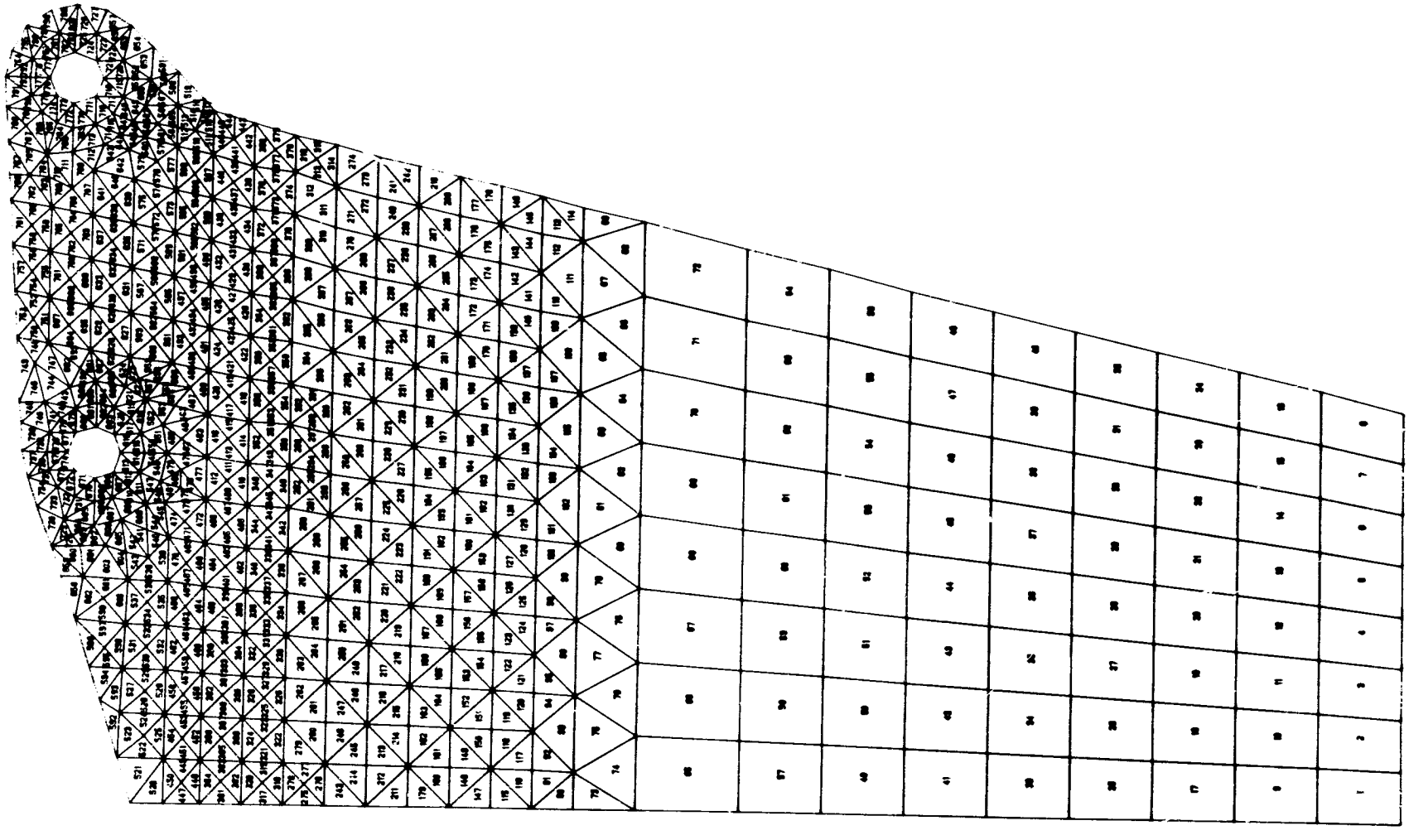

Finite Element Mesh Used in Study

Figure 6

stress levels and varying thickness distributions until a relatively uniform stress level design resulted. The variable thickness, finite element model is shown in Figure 7. Graphic comparisons of the thickness distribution shown in the last report with that resulting from the analysis described here can be made by examining Figures 8a and 8b. Similarly, comparison of the stress distribution as last reported for uniform thickness with that calculated as described above can be made by examining Figures 9a and 9b.

These finite element analyses results revealed two possible unconservative features of Berg's initial design, which may otherwise have gone undetected. First, the plate thickness around the attachment bolt holes, based on the Advanced Composite Design Guide, was not large enough to insure the desired stress levels. The more detailed modeling described here was necessary to accurately assess these stresses.

Second, there is a large stress concentration at the corner just aft of the upper bolt hole. The Berg thickness distribution shown in Figure 7 had not yet taken account of that, even after the first finite element analysis redesign.

In preparation for fabricating the first full elevator actuator attachment rib to be undertaken, step-by-step planning of the fabrication method was begun. This planning is to include the tooling, the (quasi-isotropic) composite material lay-up patterns and stacking sequence, the curing cycles and estimates of the kind of distortion and residual

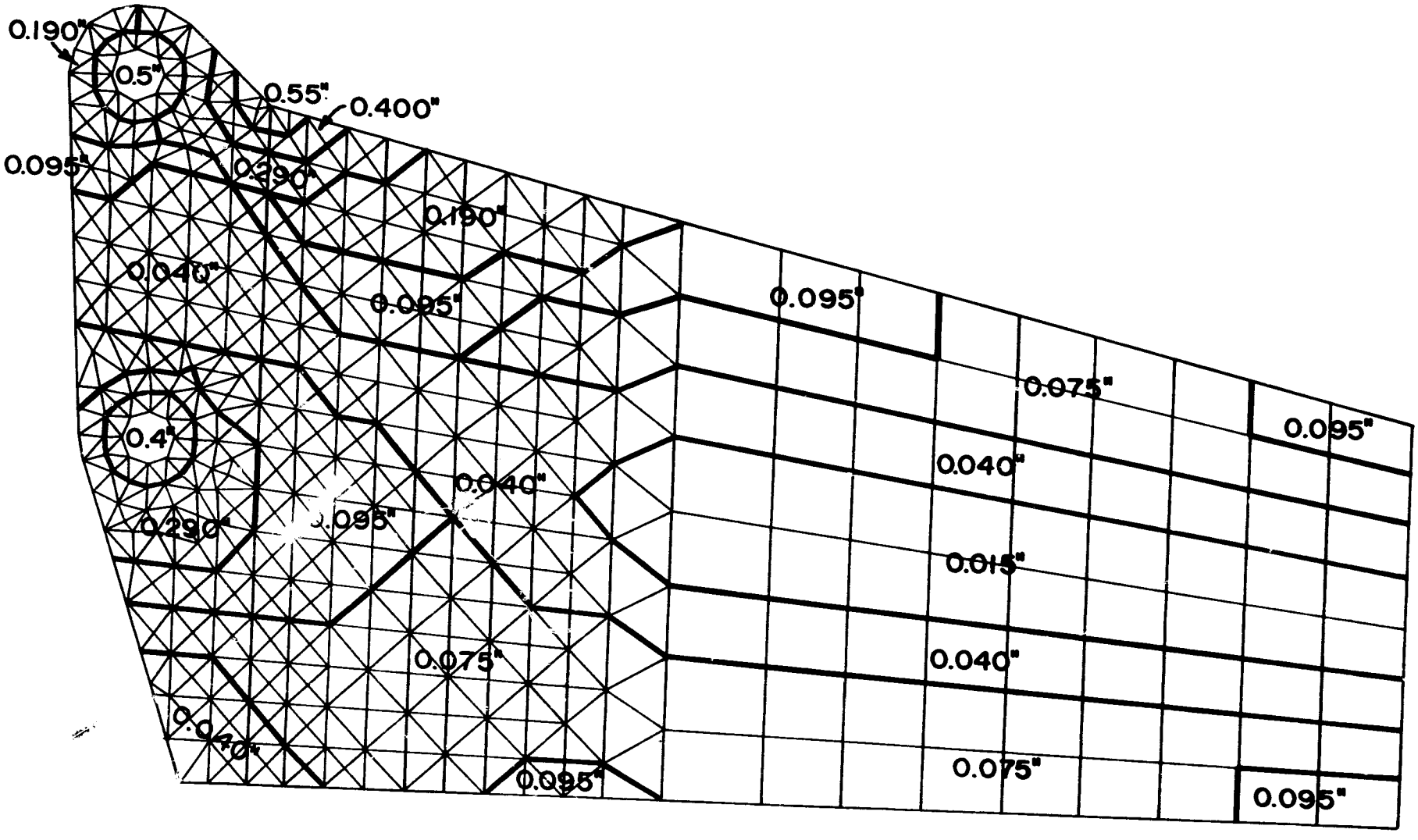

VARIABLE THICKNESS FINITE ELEMENT MESH

Figure 7

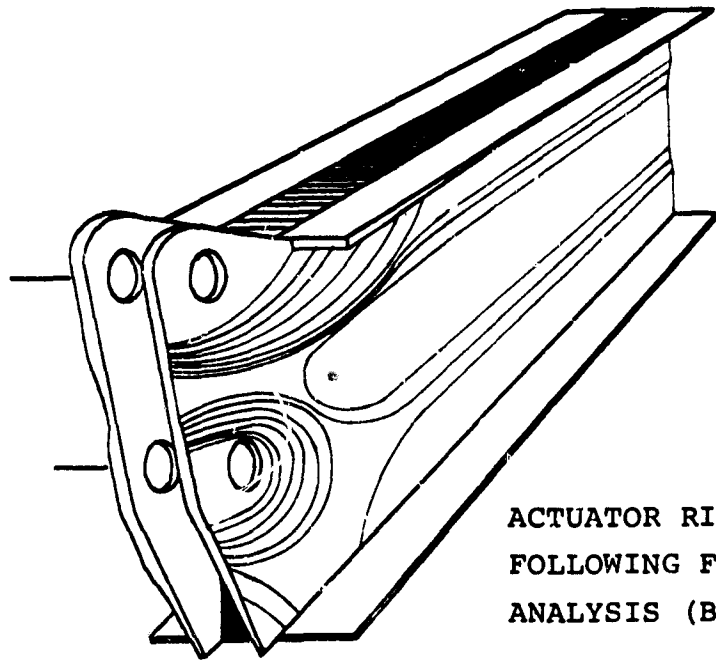

ACTUATOR RIB MODIFIED FOLLOWING FINITE ELEMENT ANALYSIS (Berg Design)

Figure 8a

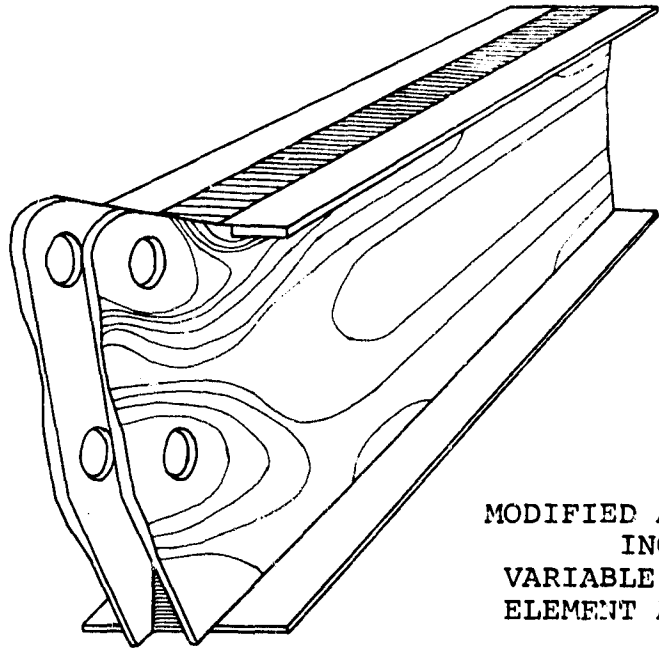

MODIFIED ACTUATOR RIB DESIGN INCOPPORATING VARIABLE THICKNESS FINITE ELEMENT ANALYSIS RESULTS

Figure 8b

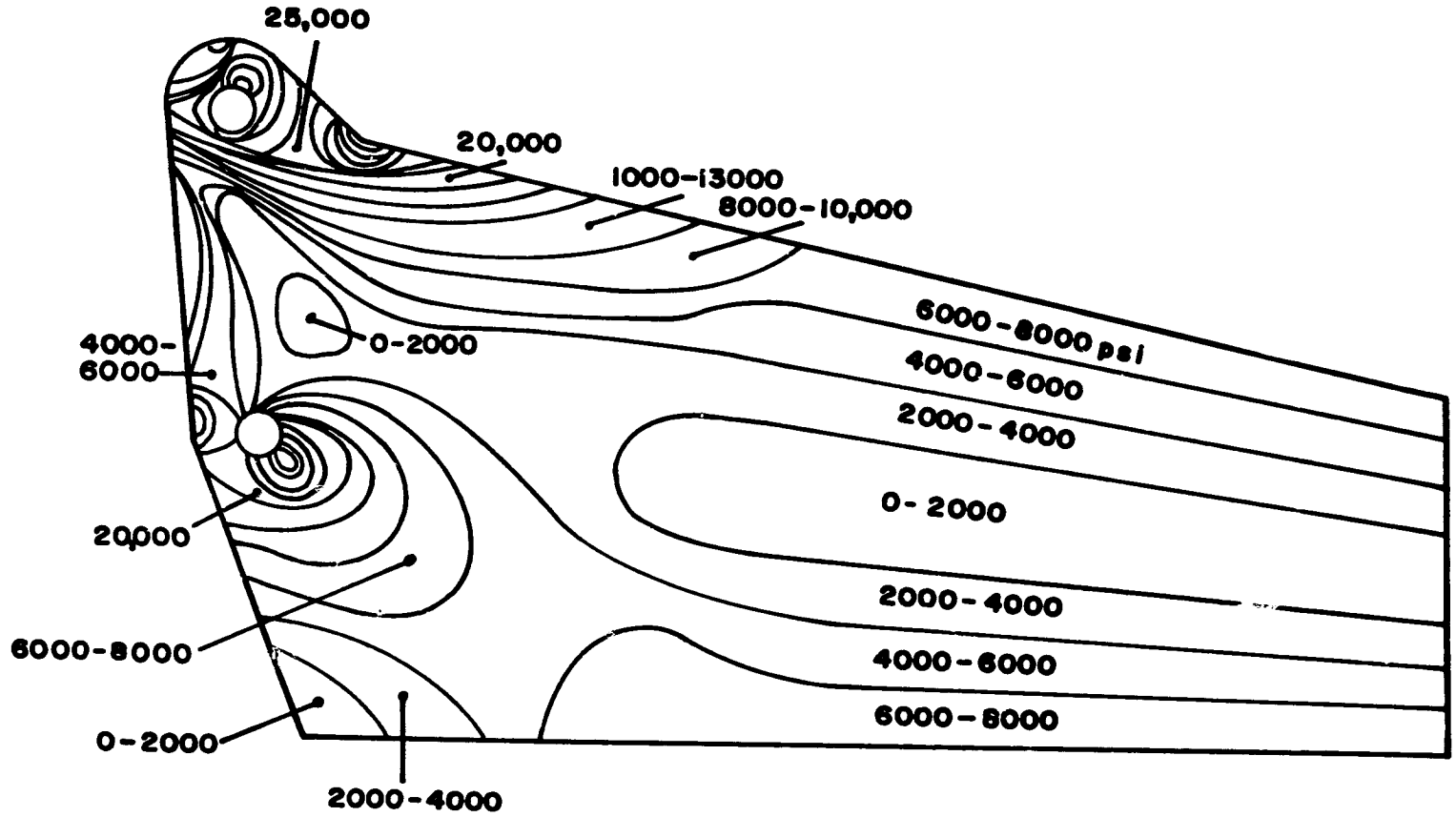

Principle Stress Contours for Uniform Thickness of 0.375 Inches

Figure 9a

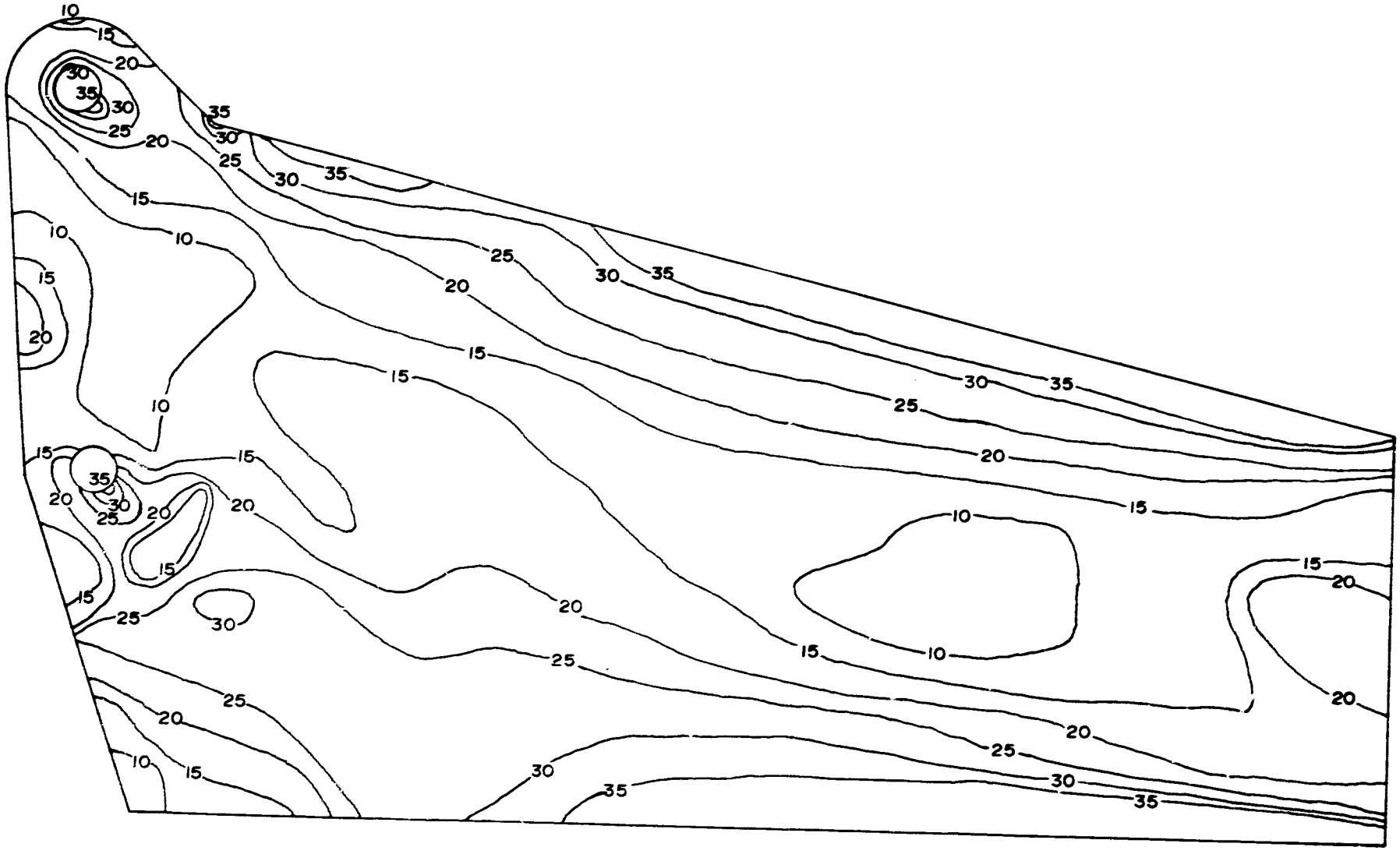

(VALUES IN KSI.)

Principle Stress Contours for Variable Thickness Mesh (of Fig. 7)

Figure 9b

stresses that would be expected to result using the proposed procedure.

In the first stages of this planning, it became clear that ease of operation and other efficiencies argue strongly for obtaining a small autoclave, just large enough to make the kinds of parts that we are considering under CAPCOMP; i.e., between one to two feet in diameter by about five feet long internally and capable of withstanding pressures in the 75 to 100 psi range. In the time that it takes to bring this new facility on line, experiments with the proposed flange-web lay-ups will be undertaken using vacuum bagging techniques, to investigate distortion problems.

3. Optimizing Fiber Orientations in The Vicinity of Heavily Loaded Joints

It has often been noted that a basic advantage of fiber-reinforced materials is the possibility of "tailoring" the material to transmit forces most efficiently. Since the number of possible material choices and fiber directions is very large, suitable methods of analysis are being developed to advance the methodology for minimizing weight in the design of attachments or joints. We have made some strides in theoretical analysis and intend to build and test some specially designed specimens. Bolted attachments involving only a single bolt are being looked at first.

Our theoretical analysis of single bolted connections will consider, at first, not-yet-optimized material arrange-

ments near the joint consisting of ordinary orthotropic graphite epoxy materials and plates with empty holes. This is being done to check the method and to compare our efforts to obtain results and the results themselves with those developed by others. The next case considered will be the loaded hole as found in connections such as the attachments of moving control surfaces. The manufacturing problem will be kept in mind, but the mechanical efficiency has priority, at least for these first stages.

As reported in previous submissions, the Muser design of the actuator rib of the B-727 elevator was based on the idea of using fibers running largely tangent to the circumference of the hole through which the forces from the actuator rod would be transmitted into the elevator structure. It is hoped that our theoretical work will lead to a new design for laminae in the region of the connector. We anticipate a lay-up pattern with fibers tangential to the circumference near the hole. From experience and from published reports (Ref. 12, 19, 20, 21 in Table V) we believe that this arrangement should result in lower stress concentrations. Our work plan has the objective of confirming this theoretically and experimentally.

It should be noted that the method of calculation being developed will be suitable only to determine stress concentration factors in the linearly elastic range. Since bearing failure occurs outside this range, calculations valid beyond

TABLE V

LIST OF REFERENCES PERTAINING TO BEARING STRENGTH OF COMPOSITES

1. Frocht, M. M. and H. N. Hill, "Stress Concentration Factors around a Central Circular Hole in a Plate Loaded through a Pin in the Hole", J. Applied Mechanics, March 1940, pp. A5-A9.

2. Dalas, Richard N., "Mechanical Joints in Structural Composites", Advances in Structural Composites, Vol. 12, Society of Aerospace Material and Process Engineers, 12th National Symposium and Exhibit, October 1967.

3. Dalas, Richard N., "Methods of Joining Advanced Fibrous Composites", Composite Materials; Testing and Design, ASTM STP 460, 1969, pp. 381-392.

4. Schjelderup, H. C. and B. H. Jones, "Practical Influence of Fibrous Reinforced Composites in Aircraft Structural Design", ASTM STP 460, 1969, pp. 285-306.

5. Waszczak, J. P. and T. A. Cruse, "Failure Mode and Strength Prediction of Anisotropic Bolt Bearing Specimens", J. Composite Materials, Vol. 5, 1971.

6. Padawer, G. E., "The Strength of Bolted Connections in Graphite/Epoxy Composites Reinforced by Colaminated Boron Film", ASTM STP 497, 1972, pp. 396-414.

7. Zurko, M. J., "Preliminary Investigation for Developing Optimum Fasteners for Joining Composite Materials", Naval Air Development Center, AD908930, February 1973.

8. Greszczuk, L. B., "Compressive Strength and Failure Modes of Unidirectional Composites", ASTM STP 521, 1973, pp. 192-217.

9. Kim, R. Y., "Effect of Temperature and Moisture on Pin-Bearing Strength of Composite Laminates", J. Composite Materials, Vol. 10, April 1976, pp. 149-155.

10. Hart-Smith, L. J., "Bolted Joints in Graphite-Epoxy Composites", NASA CR-144899, June 1976.

11. Quinn, W. J. and F. L. Matthews, "The Effect of Stacking Sequence on the Pin-Bearing Strength in Glass Fibre Reinforced Plastic", J. Composite Materials, Vol. 11, April 1977, 139-145.

TABLE V continued

12. de Jong, T., "Stresses around a Pin-loaded Hole in an Elastically Orthotropic or Isotropic Plate", J. Composite Materials, Vol. 11, July 1977, pp. 313-331.

13. Kubo, J. T., "Joints", Advanced Composites Design Guide, Vol. II, Wright-Patterson Air Force Base, 1977.

14. Collings, T. A., "The Strength of Bolted Joints in Multi-Directional CFRP Laminates", Her Majesty's Stationary Office, London, 1977.

15. Wilkins, D. J., "Environmental Sensitivity Tests of Graphite-Epoxy Bolt Bearing Properties", ASTM STP 617, 1977, pp. 497-513.

16. Eshwar, V. A., "Analysis of Clearance Fit Pin Joints", J. Mechanical Science, Vol. 20, Pergamon Press, 1978, pp. 477-484.

17. Fukuda, H., "Fastening of FRP", Unpublished Report, Aerospace Research Laboratory, Tokyo University, 1979.

18. Collings, T. A., "The Use of Bolted Connections as a Means of Joining Carbon Fibre Reinforced Plastics", Design with Fibre Reinforced Materials, Institute of Mechanical Engineers, Conference Publication, 1977-1979, pp. 29-32.

19. Puppo, A. and J. Haener, "Application of Micromechanics to Joints and Cutouts", U. S. Army Aviation Material Laboratories, TR 69-25, April 1969, AD 688168.

20. Mueller, J., "Spannungsverteilung an gelochten ueber einen Bolzen belasteten Staeben aus kohlenstoffaserverstaerktem Kunststoff", Swiss Federal Institut of Technology, Diss ETH 5546, 1975.

21. Grueninger, G., "Moeglichkeiten der Krafteinleitung in faserverstaerkte Bauteile", in: Kohlenstoff- und aramidfaserverstaerkte Kunststoffe, 1977, VDI-Verlag Duesseldorf West Germany.

the linear region would probably be necessary, and suitable failure criteria would have to be established before there can be hope for good agreement between analysis and test results. We expect this sort of work to wait till late spring because the construction of the test specimens, their testing and the linear analytical work will require all the time available until then.

4. Supporting Development of Mechanical Joints

The work of graduate student Wonsub Kim and, until August, of Research Associate Kiyoshi Kenmochi, in this period, concentrated on the interpretation of bearing failure test and photoelastic results in pin-loaded composite tension specimens. This followed from our conclusion that designing a mechanical joint to fail in bearing makes the best use of strength. Reducing fastener diameter increases a given joint's tensile strength and to a first approximation leaves shear strength unaffected, but bearing stress is ultimately limiting in this process. For this reason, we have concentrated on bearing strength and bearing failure mechanisms in this research.

To place the results we obtained in perspective, a literature survey was made of experimental and theoretical work published in this area. This survey has shown that within the substantial literature of composite materials, relatively few research results connected with mechanical joining problems have been published. Furthermore, among those reported

works which do exist many are inconclusive and others are not mutually consistent. A total of 21 references which seem pertinent are listed in Table V on pages 30-31 and a summary of the most important results, from the point of view of this study, follows.

Summary of the Literature Survey

A. General

1) There are relatively few publications available dealing with bearing failure in composite materials.

2) Among such publications as do exist the work reported is roughly 90% experimental, 10% theoretical.

B. Theoretical Work

1) The most pertinent work appears to be that of T. de Jong (12)* and V. A. Eshwar (16). Both are two dimensional theories and assume infinitely rigid pins. Neither includes the effect of friction, comparisons with experiment nor satisfies boundary conditions exactly.

2) T. de Jong shows marked effects of ply orientations on stress distributions, but provides no estimates of the inaccuracies introduced by failure to meet displacement boundary conditions on the hole.

---

* Numbers in parentheses in this section correspond to reference numbers in Table V, pages 30-31.

3) V. S. Eshwar's work is limited to isotropic materials but, by using an inverse procedure specifying displacements and then solving for the corresponding loads on the hole, shows that the boundary conditions can be met to within satisfactory accuracy. Among his results are the following:
   a) The area of contact between pin and plate has an asymptotic relation to load limited by Poisson's ratio, for example, to 166° (compared to 180°) for $\nu = .3$.
   b) Non-linear behavior of maximum stresses with load are exhibited (concave downward) as a result of increasing contact area with load.
   c) The distribution of radial stress, however, changes only slightly with load and is well approximated by $\sigma_r = \sigma_{r_{max}} \left[1 - \left(\frac{\theta}{\theta_c}\right)^2\right]^{\frac{1}{2}}$, where θ_c is the angular position of the edge of contact measured from the axis of symmetry.
   d) The effect of the third direction is likely to be great near the hole and suggests caution regarding use of 2-D theory in formulating failure criteria.

C. Photoelastic Studies

Stress concentration factors determined by Frocht and Hill (1) were found to vary as follows:

1) If the ratio of the diameter of the hole to the width of the plate, D/t increases, the stress concentration factor decreases.

2) If the clearance between pin and hole increases, the stress concentration factor decreases.

3) If the number of pins increases, the stress concentration factor decreases.

4) The effect of lubrication between pin and hole is measurable but very small (thus validating the assumption of no friction between pin and hole in mathematical analyses).

D. Experimental Work

1) All referenced works investigate the effects of one or more of the following six factors.
   a) Fiber orientation
   b) Stacking sequence
   c) Ratio of hole diameter to plate thickness (D/t)
   d) Clamping force
   e) Environmental condition
   f) Local reinforcement of the hole

2) All tests used virtually the same method, i.e., apply load to the pin until failure occurs.

3) Of ten references reporting the effect of fiber orientation, four (3, 8, 15, 18) reported the effect to be great, five (2, 9, 10, 14, 17) pronounced the effect small and one (13) was noncommital.

4) Two (9, 13) of three investigations reported environmental factors as important influences, but one (15) found them of no significance.

5) All three of those reporting stacking sequence effects (11, 14, 18) concluded it is relatively large (But two of these were written by the same author.).

6) Four (10, 13, 14, 18) out of six papers reported clamping force as having a large influence on bearing strength. The remaining two authors (3, 7) pointed out that the significant fact is the existence of clamping force, not the amount of such force.

7) Five investigators tested the effect of D/t; one (14) reported it as big, two (15, 17) as small, and two (2, 13) found their tests inconclusive.

8) Three authors (2, 6, 10) investigated the influence of local reinforcing around the hole using colaminated third materials, and they all reported the effect to be favorable and very large.

9) Two reports (5, 13) mention the effect of clearance between pin and hole, but it was only calculated using a Finite Element Method.

The results of RPI's testing is presented in this section in some detail and is also related to the corresponding data found in the literature search. Table VI summarizes RPI bearing test results to date. Analysis of the photoelastic test results hasn't been completed. Some initial

TABLE VI

RESULTS OF RPI BEARING TESTS

Specimen* Designation	Specimen Thickness (inch)	Load Maximum (lbs)	Bearing Strength (psi)	Strength Ratio to that of Specimen E
Type A**				
-1	0.085	1,240(2)	58,353	0.82
-2	0.083	1,500	73,764	0.94
Type B				
-1	0.094	1,610	68,510	0.97
-2	0.094	1,725	74,902	0.95
Type C				
-1	0.095	1,445	60,842	0.86
-2	0.095	1,625	69,817	0.89
-3 HSS(1)	0.095	1,120	47,158	0.60(3)
Type D				
-1	0.085	1,400	65,882	0.93
-2	0.086	1,310(2)	62,173	0.79
Type E				
-1	0.083	1,470	70,843	1.00
-2	0.083	1,600	78,682	1.00
Photoelastic	0.089	2,750	61,798	0.72
" "	0.095	3,350	70,526	0.82
" "	0.089	3,100	69,663	0.81
" "	0.085	3,650	85,882	1.00

---

*Specimen Types A-E have holes with ¼ inch diameter. The hole diameter in the photoelastic specimens is ½ inch.

**The specimen designations are interpreted as follows:

Type A	{0°/90°}8s	Type D	{±45°/0°/90°}4s
Type B	{±45°/0°}6s	Type E	{±45°/±22.5°/±67.5°/0°/90°}2s
Type C	{±45°/90°}6s		

(1) Hole drilled with high speed steel drill bit.

(2) Found to be premature failure.

(3) Ratioed to Case E-2.

conclusions, however, can be drawn; namely,

A. The material behaves as if almost perfectly elastic until just in the vicinity of the maximum load. Through both the unloading and loading process the charting pen follows exactly the same curve of load vs displacement. Even after the unloading and loading process, the photoelastic fringes were identical to those observed before this process. The behavior close to the failure load could not be checked by these means.

B. Stress distributions are quite different from one fiber orientation type to another (see Figure 10). On the other hand, the values in Table VI do not always confirm the photoelastic insights. "Scatter" between the duplicate specimen pairs is large enough to almost obscure differences, but specimen Type E, which is closest to isotropy, showed the highest strength; Type B looks next best; and Types A, C and D seem roughly the same and least good. Since hole diameter to specimen width varied slightly between the photoelastic and other specimens, it may be best to consider bearing strength averages based only on non-photoelastic tests. Then the strength of lay-up Type E is around 75 Ksi. The lowest average would be that of Type C at 65 Ksi. This way of looking at the data makes the maximum variation of bearing strength less than 12%. Hence, contrary to what would be expected from photoelastic results, such as shown in Figure 10, the pin-bearing strength does not change greatly from one fiber orientation to another. Two exceptions to this statement are specimens which failed prematurely.

Type E; 16 layers

$\{\pm 45^{\circ}/\pm 22.5^{\circ}/\pm 67.5^{\circ}/0^{\circ}/90^{\circ}\}2s$

Load 2,500 lb

Type C; 18 layers

$\{\pm 45^{\circ}/90^{\circ}\}6s$

Load 2,500 lb

Type A; 16 layers

$\{0^{\circ}/90^{\circ}\}8s$

Load 3,000 lb

Isochromatic fringe patterns for various fiber orientations

Figure 10

Tables VII and VIII relate the RPI results to those in the literature. Table IX represents an attempt to draw conclusions as to fiber orientations which constitute good design for bearing strength by making comparisions selectively among the results reported in the literature and those of the RPI tests reported here. Since materials varied from test to test, bearing failure loads are normalized to particular ply orientations. While hardly conclusive, the following tentative conclusions can be drawn:

A. Combinations including 0° and ±45° plies have superior bearing strength. (Comparisons 2, 3 and 4 in Table V)

B) Having 90° plies provides questionable benefits. (Comparison 2 and 4)

C) Clamping does not alter the relative strength between 0/90 and 0/±45 plies. (Comparison 2)

D) Clamping does seem to alter the relative strength between 0/±45 and 90/±45 plies. (Comparison 4)

E) Changing fiber material may alter the relative strength between 0/90 and ±45 plies. (Comparison 1, assuming conclusion C) holds also for those ply comparisons)

An interesting conclusion from our testing is that the bearing strength does not seem to be a strong function of the ratio of the diameter of the hole to the thickness of the plate. This is contrary to results presented in Reference 14. This D/t ratio for photoelastic specimens was roughly

TABLE VII

SUMMARY OF PIN BEARING TESTING

REFERENCES	MATERIAL	EFFECT OF FIBER ORIENTATION	EFFECT OF MOISTURE & TEMP.		EFFECT OF STACKING SEQUENCE	EFFECT OF CLAMPING FORCES	EFFECT OF D/T		REMARKS
			CONDITIONS	CONCLUSIONS			VALUES	CONCLUSIONS	
2.* DALAS	S-GLASS/ EPOXY	"SMALL"	–	–	–	–	–	NOT CLEAR	INTERLAYER LAMINAE IMPROVE THE STRENGTH
3. DALAS	BORON/ EPOXY	"SIGNIFICANT"	–	–	–	"SMALL"	–	–	BOLTING HAS NO EFFECT ON ADHESIVE JOINT
4. SCHJELDERUP	BORON/ EPOXY	–	–	–	–	–	.52 TO 1.56	(SEE REMARK)	NO EFFECT ON SHEAR AND TENSION FAILURE
6. PODAWER	G/E (FIBER-COURTAULDS TYPE HT-S) (CIBA EPN 1138)	"VERY BIG" (SEE REMARK)	–	–	–	–	–	–	ADDING BORON FILM REDUCED EFFECT OF ORIENTATION
7. ZURKO	G/E (NAMCO 5206)	–	–	–	–	"SMALL" (SEE REMARK)	–	–	BUT THE EXISTENCE OF SOME CLAMPING IS IMPORTANT
9. KIM	G/E	"SMALL"	RM. DRY TO 260° SATUR-ATION	"BIG"	–	–	–	–	–
10. HART-SMITH	G/E	"SMALL"	–	–	–	"BIG"	–	–	COLAMINATED GLASS LAYER IMPROVES STRENGTH
11. QUINN	GLASS/ EPOXY	–	–	–	"BIG"	–	–	–	–
13. KUBO	G/E (NAMCO 5206)	(SEE REMARK)	-100°F TO 375°F	"BIG"	(SEE REMARK)	"BIG"	–	(SEE REMARK)	WIDE SCATTER AMONG DATA POINTS
14. COLLINGS	G/E (HTS/(ERLA4617/DOM))	"SMALL"	–	–	±15%	"BIG"	1.0 TO 4.2	"BIG"	–
15. WILKINS	G/E (NAMCO 5208/T300)	"BIG"	RM. DRY TO 250° SATUR-ATION	"NOT SIG-NIFICANT"	–	–	5.6 TO 6.8	"SMALL"	–
17. FUKUDA	GLASS/ EPOXY	"SMALL"	–	–		–	2.4 TO 4.8	"SMALL"	–
18. COLLINS	G/E	"BIG"	–	–	"BIG"	"BIG" (SEE REMARK)	–	NOT CLEAR	HAS UPPER LIMIT
RPI	G/E	"SMALL"	–	–	–	–	2.7 TO 5.5	"SMALL"	–

* THESE NUMBERS REFER TO THE LIST OF PAPERS IN TABLE V

TABLE VIII
BEARING STRENGTH WITH VARIOUS FIBER ORIENTATIONS

References	Clamping (Force, Pressure, Torque)	{0°/90°}s	{0°/±60°}s	{±45°}s	{0°/±45°}s	{90°/±45°}	{0°/90°/±45°}
2. Dalas	Not clear	0°-80.2 Ksi, ±45°-75.4 Ksi, 90°-72.4 Ksi*					
3. Dalas	Not clear	-	74 Ksi	-	-	-	-
6. Pawader	(200 lb)	-	-	47.9 Ksi (1.0)**	81.7 Ksi (1.7)	-	-
9. Kim	None	-	-	-	85.1 (1.0)	74.8 (0.88)	89.8 (1.06)
10. Hart-Smith	None	Maximum variation; 12%					
13. Kubo	Not clear	-	-	-	-	-	-
14. Collings	3.2 Ksi	116.0 (1.0)	128.4 (1.11)	121.0 (1.04)	130.4 (1.12)	-	-
15. Wilkins	(5 lb-in.)	-	-	-	122.7 (1.0)	63.1 (0.51)	-
17. Fukuda	None	42.3 (1.0)	-	50.6 (1.20)	-	-	-
18. Collings	Not clear	Reported as ±30% variation					
RPI	None	58.4 (1.0)	-	-	68.5 (1.17)	60.8 (1.04)	65.9 (1.13)

* Note: Unidirectional lay-ups.

** Numbers in parentheses are normalized to a particular value across table rows.

TABLE IX

NORMALIZED BEARING STRENGTH COMPARISONS AMONG REFERENCE DATA AND FROM RPI WORK TO DETERMINE THE EFFECT OF FIBER ORIENTATIONS

Comparison Number	Fiber Orientation			
1.		Ref. No. --	14*	17
		Mat'l. --	G/E	Glass/E
	{0/90}s		1.0	1.0
	{±45}s		1.04	1.2
2.		Ref. No. --	14*	RPI
		Mat'l. --	G/E	G/E
	{0/90}s		1.0	1.0
	{0/±45}s		1.12	1.17
3.		Ref. No. --	14*	6**
		Mat'l. --	G/E	G/E
	{±/45}s		1.0	1.0
	{0/±45}s		1.08	1.7
4.		Ref. No. --	9	15***	RPI
		Mat'l. --	G/E	G/E	G/E
	{0/±45}s		1.0	1.0	1.0
	{90/±45}s		0.88	0.51	0.89
	{0/90/±45}s		1.06	--	0.97

*3.2 Ksi clamping; **200 lb clamping; ***"5 lb-in on a screw" clamping.

5.6 and for the bearing coupons was 2.8, yet the corresponding bearing strengths were quite close. With such ratios, according to Reference 14, the bearing strength of the photoelastic specimen should be lower than the bearing test coupon by at least 50%, but this series of tests at RPI shows that the photoelastic specimens have strengths which are even slightly higher.

5. Failure Mechanisms

Some of the specimens tested to failure in our program were cut along the center line passing through the two holes so as to allow microscopic investigation through the specimen thickness in the area of the failure.

After very careful polishing, the cut edges were inspected both on the failed area of the hole as well as on the unfailed side. Microscope magnification factors of 25 and 50 were used. With the magnification factor of 50, the cracks on the damaged area as well as each layer of fiber orientation could be seen clearly. Figure 11 shows the cracks on failed specimens with several typical fiber orientations. These pictures were taken with a magnification factor of 25.

It seems clear that the cracks started at an arbitrary point on the loaded edge of the hole and ran across the layers, even through the 0° layers, in a direction roughly ±45° to the laminae. This kind of crack has been observed often

Type A

(Hole drilled with carbide tipped drill bit)

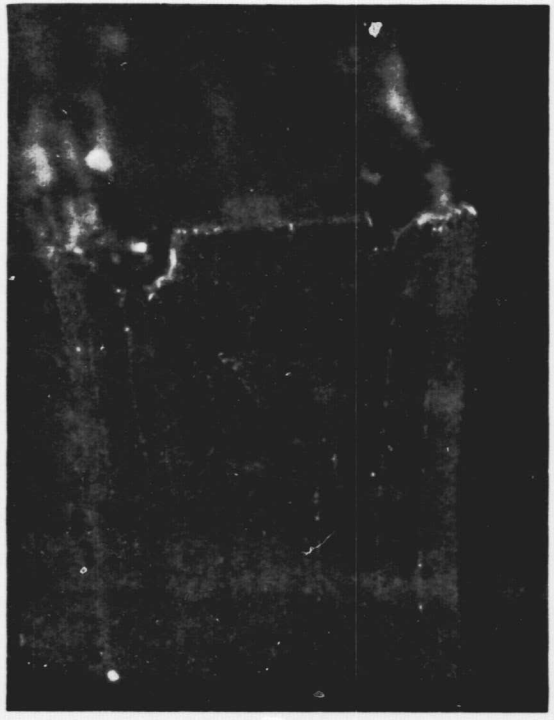

Type C

(Hole drilled with carbide tipped drill bit)

Type C

(Hole drilled with high speed steel bit)

Cracks within the laminates following bearing failure (Magnification25)

Figure 11

in tests of brittle isotropic materials loaded in compression. If these cracks are along shear lines as they appear to be and as they are in compression tests of isotropic materials, then shear in a direction transverse to the plane of the plate should be investigated and regarded as an important factor in the bearing failure of composite materials.

6. Special Delamination Studies

The effect of delamination on the bearing strength of a composite material seems to be much more severe than it is on other material allowables. In a brief investigation of this effect two additional specimens were prepared using exactly the same procedures as those used in all the other tests. In this case, however, the holes were purposefully drilled with a high speed steel drill bit instead of a carbide tipped drill bit. Every dimension and process of preparation was identical except the drill bit used. As expected these holes were flawed to a greater extent than those drilled with a carbide tipped bit. The thickness of the plates around these holes was increased by up to one thousandth of an inch. This indicates that delaminations were induced by drilling with the high speed steel bit. These holes were investigated further using ultrasonic NDE techniques.

Figure 12, showing ultrasonic transmission loss images of the delamination around holes drilled with a high speed steel bit and with a carbide tipped bit, shows the former to

Type C - Hole drilled with carbide tipped bit

Delaminations occurred on right-upper side of the hole.

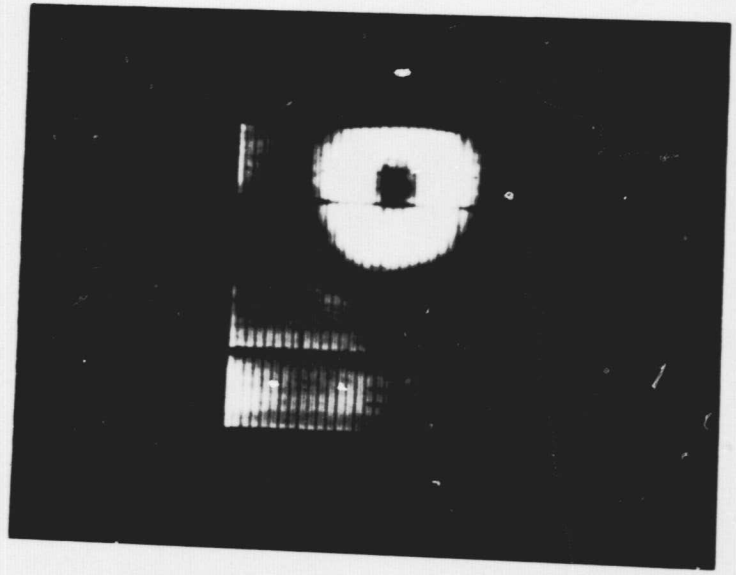

Type C - Hole drilled with high speed steel bit

Delaminations occurred all around the hole.

Ultra-sound transmission-loss images prior to loading. (Pictures show that delaminations are more severe around hole drilled with a HSS drill bit than when drilled by a carbide tipped drill bit.)

Figure 12

be more extensive. Note that the technique does not yet allow interpretation of delamination as a function of depth, but only of area around the hole in the plane of the laminae.

These two specimens were tested using the same process as described above. A mishap failed one specimen of lay-up Type A ($\{0°/90°\}_{3s}$) before useful data could be taken. Specimen Type C ($\{\pm45°/90°\}_{6s}$), however, was tested successfully. It showed much less strength than the same specimen with higher hole quality, as expected. This result is also included in Table II.

These special tests lead to the following conclusions:

1) Holes drilled with carbide tipped bits have delamination like that caused by high speed steel bits, only less of it.
2) The amount of delamination caused by drilling affects the bearing strength of a joint substantially.
3) Preventing or compensating for delamination in some way can improve the bearing strength of a joint greatly. The large and favorable effect of clamping seems to stem from this phenomenon.

PART II

CAPGLIDE (Composite Aircraft Program Glider)

CAPGLIDE (Composite Aircraft Program Glider)

(R. J. Diefendorf, H. J. Hagerup, G. Helwig)

CAPGLIDE is an undergraduate program to design, build and test advanced composite structures. Students will obtain direct "hands-on" experience in advanced composite structures which can serve as a springboard for the more sophisticated CAPCOMP projects. In dealing with the design of a complete vehicle, the effect of any given change on other aspects must be dealt with. In this way the project also requires students majoring in aeronautical, mechanical and materials engineering to interact in much the same way as they do in industry.

An ultra-light sailplane was selected as the first demonstration project because a full scale flight vehicle would maximize student interest and would be of relative simplicity and low cost to build. A conventional layout monoplane with three-axis control resulted in the following estimated performance:

1) Stall speed, 15 knots,
2) Best glide ratio, 17 and
3) Minimum sink rate, 2.0 feet per second.

While the glide ratio of the ultra-light sailplane is similar to that of post World War II utility gliders, the more important sink rate is in the range of standard class sailplanes.

The major activity during the current reporting period was the manufacture and assembly of the glider. The fuselage-booms were built first. Parallel to this, the wing-skins were laid-up on a flat polyethylene-surfaced table and subsequently curved to shape in wing molds. This two step method (see Figure 13), consisting of (1) semi-curing on a flat table and (2) final curing into shape in molds, was very successful.

Step 1. Flat lay-up on polyethylene plate.

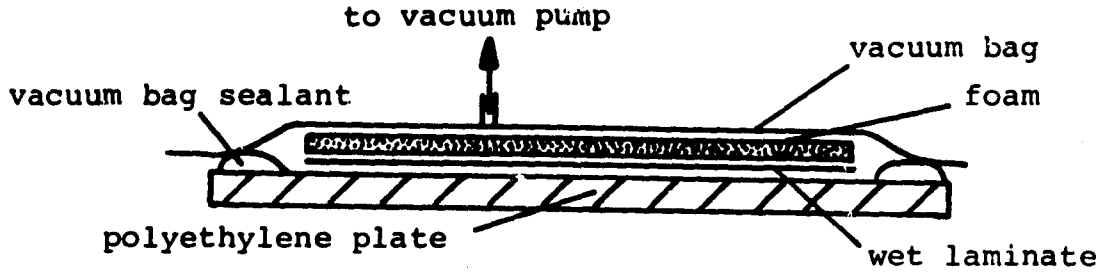

Step 2. Lay-up in mold.

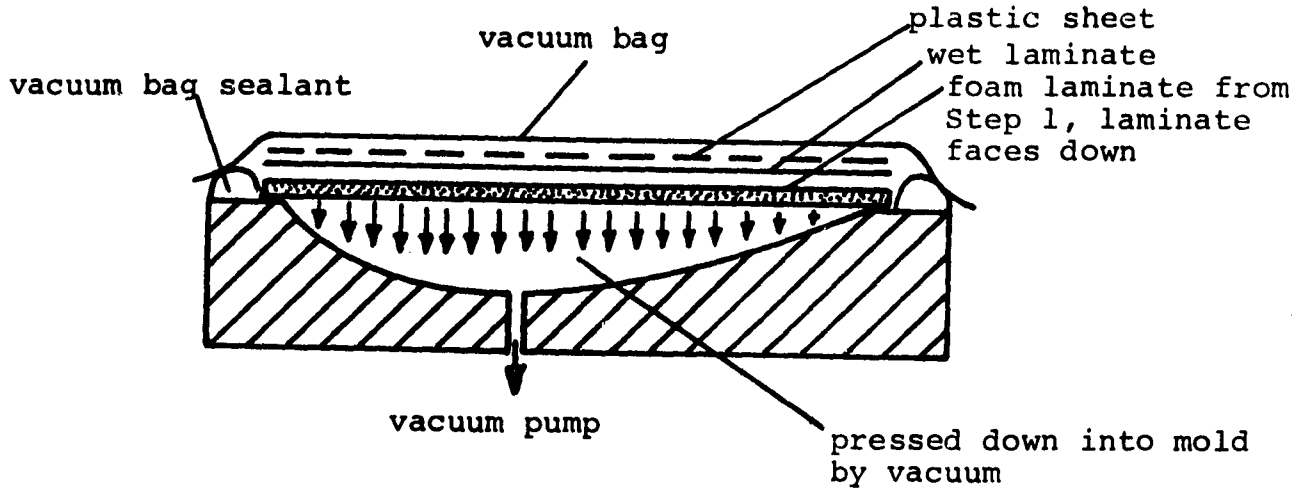

Wet-Lay-Up Mold Technique

Figure 13

Before the cap-strips of the wing spars were manufactured, a test spar, which was built earlier, was loaded to destruction. A test loading jig was hung from a crane and was used to introduce the forces at four points into the cantilevered spar (see Figure 14).

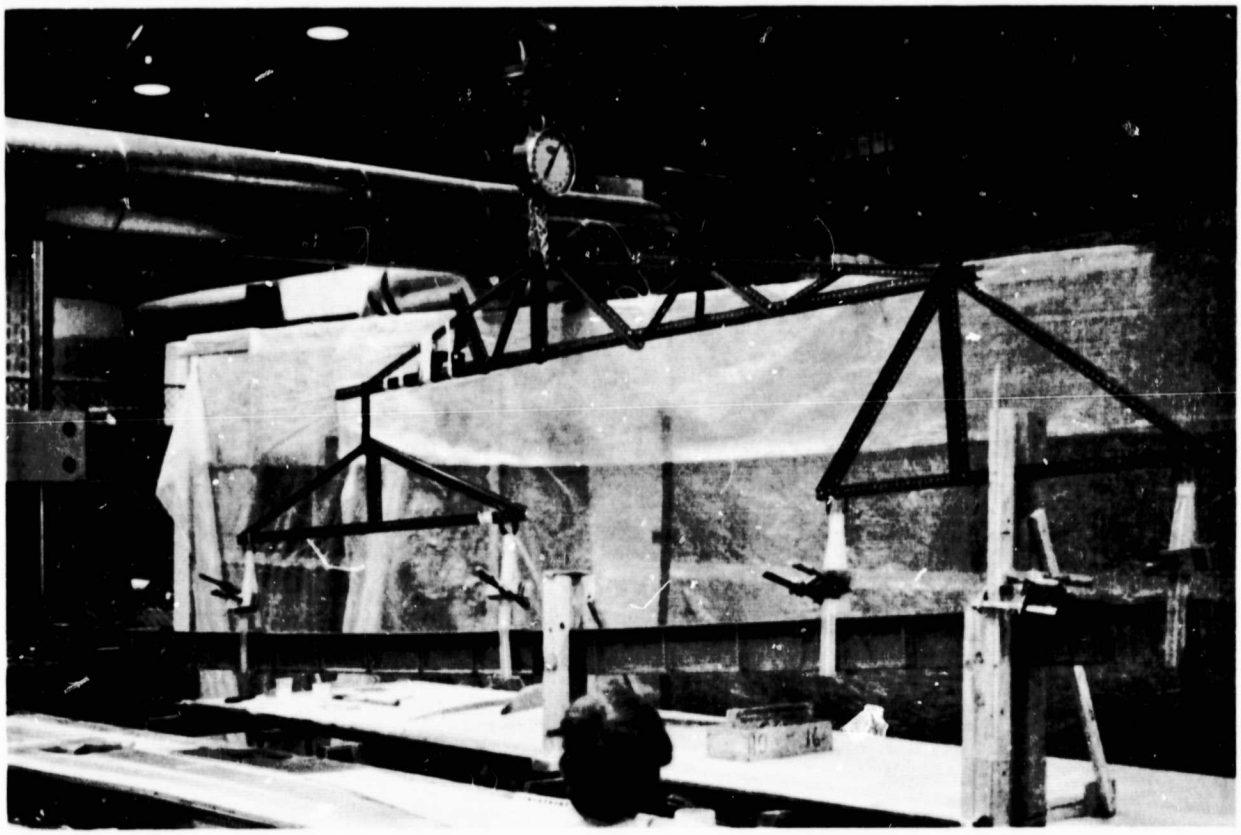

Figure 14 Spar Test

The cantilever point was achieved by clamping with the connection from the other wing. The wing-connection was, therefore, tested in the same process. Special guides were necessary to prevent the I-beam spar from twisting, and these can also be seen in Figure 14. In the first attempt, the loading jig failed at 50% of the ultimate load (i.e., design load with safety factor of 1.5), and the test spar was damaged and

had to be repaired. The next test was successful. The spar failed in the connection with a safety factor slightly over 1.5. The nature of the failure was graphite capstrips splitting under shear forces. The actual wing connection will be reinforced to prevent shearing-off of the I-beam flanges. A still higher safety factor can, therefore, be expected. A 3-foot wing section, previously tested for wing-skin buckling, was tested again at an elevated temperature of about 125°F. Significant stiffness loss was obvious. Accordingly, the wing was reinforced with two additional webs from the root to the inboard end of the ailerons, which added some extra weight.

The tail was built with single-sided, Kevlar-stabilized foam sheets. These sheets were then bent to the rib framework. This technique, again, was simple and effective in producing true-to-tolerance airfoil shapes with an extremely lightweight structure.

From the following Figures, 15-18, the construction details and materials actually used in fabricating the glider can be seen. The actual weight of the parts is also listed. Weights of major components sub-assemblies are shown in Table X. Figures 19-21 are photographs which show various assemblies of the first CAPGLIDE aircraft, RP-1, in different stages of completion; Figure 19 is the tail assembly, Figure 20 is a semi-span wing substructure and Figure 21 is the fuselage.

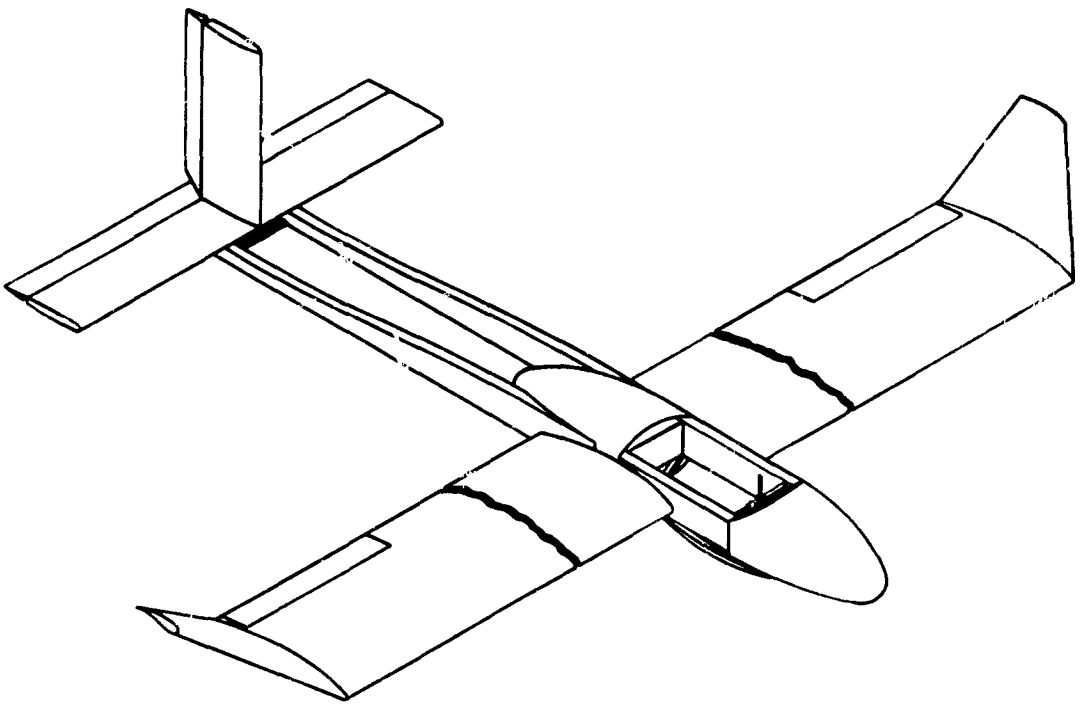

Figure 15 RP-1

CAPGLIDE
RENSSELAER POLYTECHNIC INSTITUTE NOVEMBER 1979

Item	Units		
Span	m(ft)	11.5	(37.7)
Length	m(ft)	5.78	(18.9)
Height	m(ft)	1.28	(4.2)
Wing area	$m^2(ft^2)$	12	(129.0)
Aspect ratio	-----	11	-----
Wing section profile	-----	FX-63-137	-----
Vertical stabilizer			
Area	$m^2(ft^2)$	0.72	(7.8)
Span	m(ft)	1.2	(3.9)
Profile	-----	FX-L-111-142	-----
Horizontal stabilizer			
Area	$m^2(ft^2)$	1.8	(19.4)
Span	m(ft)	3.0	(9.8)
Profile	-----	FX-L-111-142	-----
Performance with 120 kg			
Stall speed	km/h(mph)	36	(22.5)
Minimum sink rate	m/s(ft/s)	0.62	(2.0)
at	km/h(mph)	40	(25.0)
Maximum glide-ratio	-----	20	-----
at	km/h(mph)	52	(32.5)
Empty weight	kg(lbs)	52.9	(116.3)
Tail control effectivenesses			
V/V^* Horizontal	-----	0.41	-----
V/V^* Vertical	-----	0.057	-----

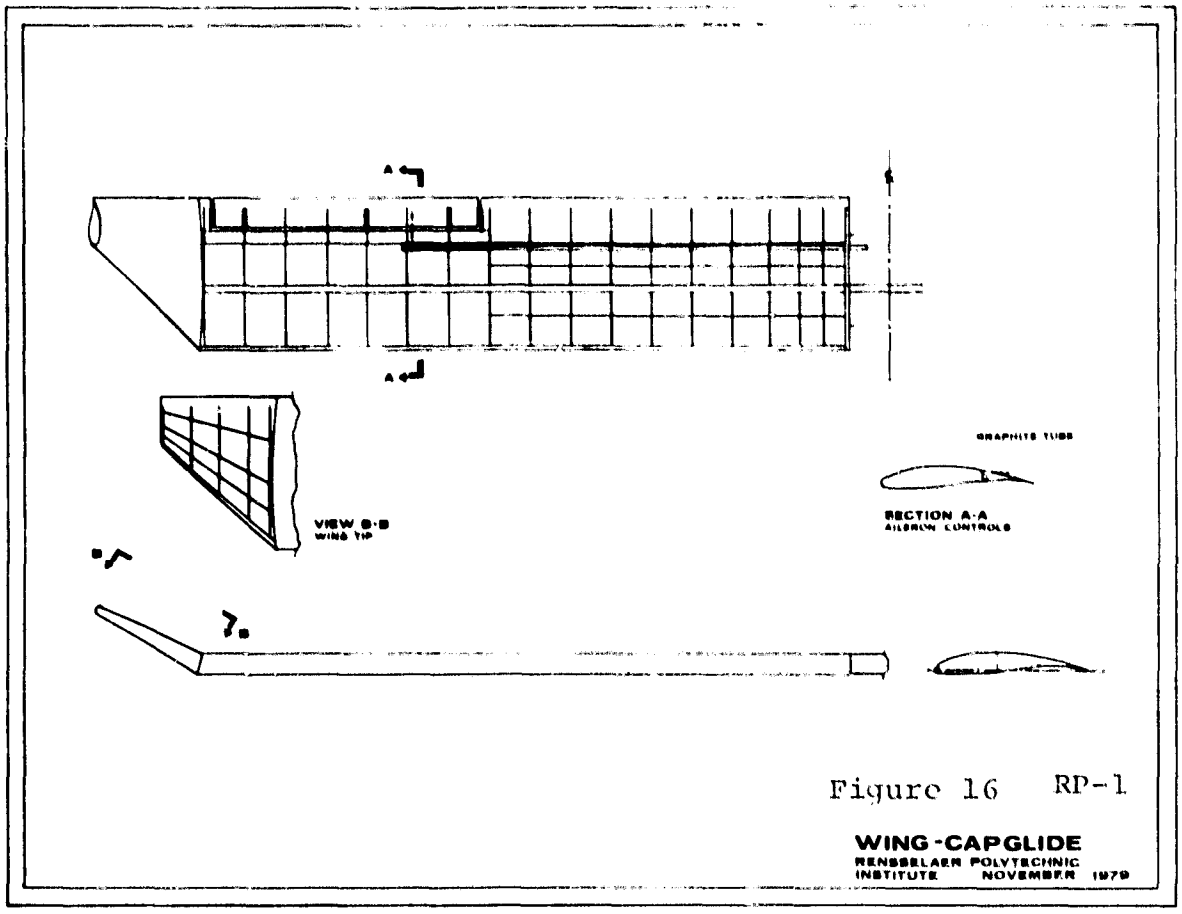

Figure 16 RP-1

Part	Materials	Weight (g)
2 Spar capstrips	Graphite	1,600
Main web	Kevlar, foam	700
17 Ribs	Glass, foam	1,020
2 Skins	Kevlar, foam	6,580
Front web	Glass, foam	140
Reinforcement webs	Glass, foam	340
Back web	Glass, foam	83
Root rib	Graphite, foam, spruce	750
Wing connection	Graphite, plywood, foam	500
Aileron tube	Graphite	220
Hinges	Graphite	100
Wing tips	Kevlar, foam	900
Leading edge	Balsa	500
		13,433
Resin for bonding		2,600
	Total =	16,033

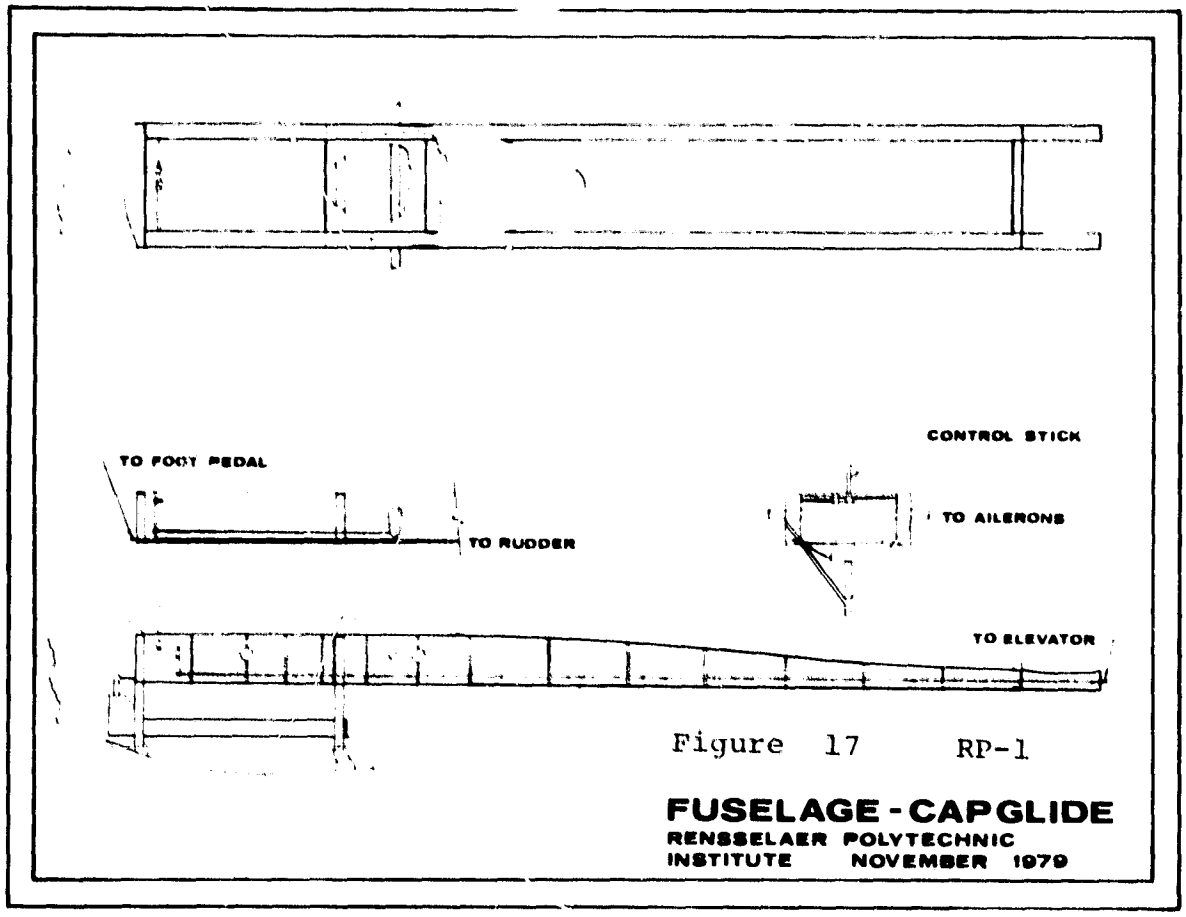

Figure 17 RP-1

Part	Materials	Weight (g)
4 Boom capstrips	Graphite	3,000
4 Webs	Kevlar, foam	3,400
Stiffeners	Kevlar, foam	200
Fuselage	Kevlar	900
Pilot beam	Graphite, balsa	1,300
Landing skid	Glass, spruce	1,100
4 Wing supports	Spruce	320
Push Rods	Aluminum	500
Aileron Tube	Graphite	80
Cranks	Graphite	100
Control stick	Graphite	120
4 Landing struts	Graphite, balsa	600
2 Connections blocks	Spruce	140
Torsion box	Graphite, foam	810
3 Boom connections	Graphite, balsa	200
8 Filler blocks	Spruce, balsa	280
		13,050
Resin for bonding		2,500
	Total =	15,550

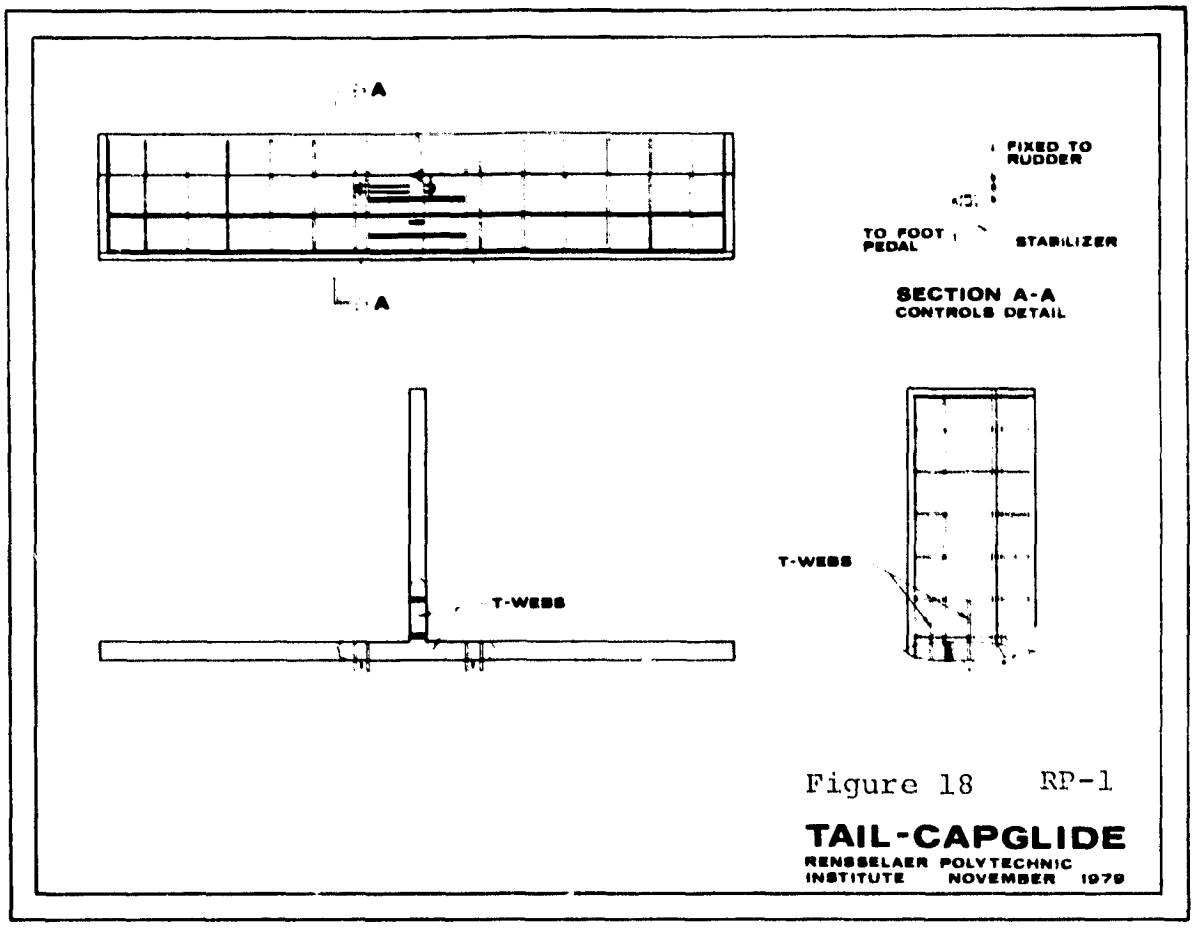

Figure 18 RP-1

Part	Materials	Weight (g)
Skins	Kevlar, foam	3,000
24 Ribs	Foam	144
Web (horizontal)	Kevlar, foam	192
Web (vertical)	Kevlar, foam	96
2 Capstrips	Graphite	225
4 Rudder Webs	Foam	54
11 Hinges	Graphite	220
Rudder connection	Graphite, tube	150
Leading edge	Balsa	135
Wing tips	Balsa	90
2 T-Webs	Kevlar, foam	128
Tail connection	Graphite	50
		4,484
Adhesive		600
	Total =	5,084

TABLE X

CAPGLIDE: RP-1 ACTUAL TOTAL WEIGHTS

	(kg)	(lbs)
Wings	32.2	70.8
Tail	5.1	11.2
Fuselage	15.6	34.3
Total Weight	52.9	116.3

Figure 19 Tail Assembly

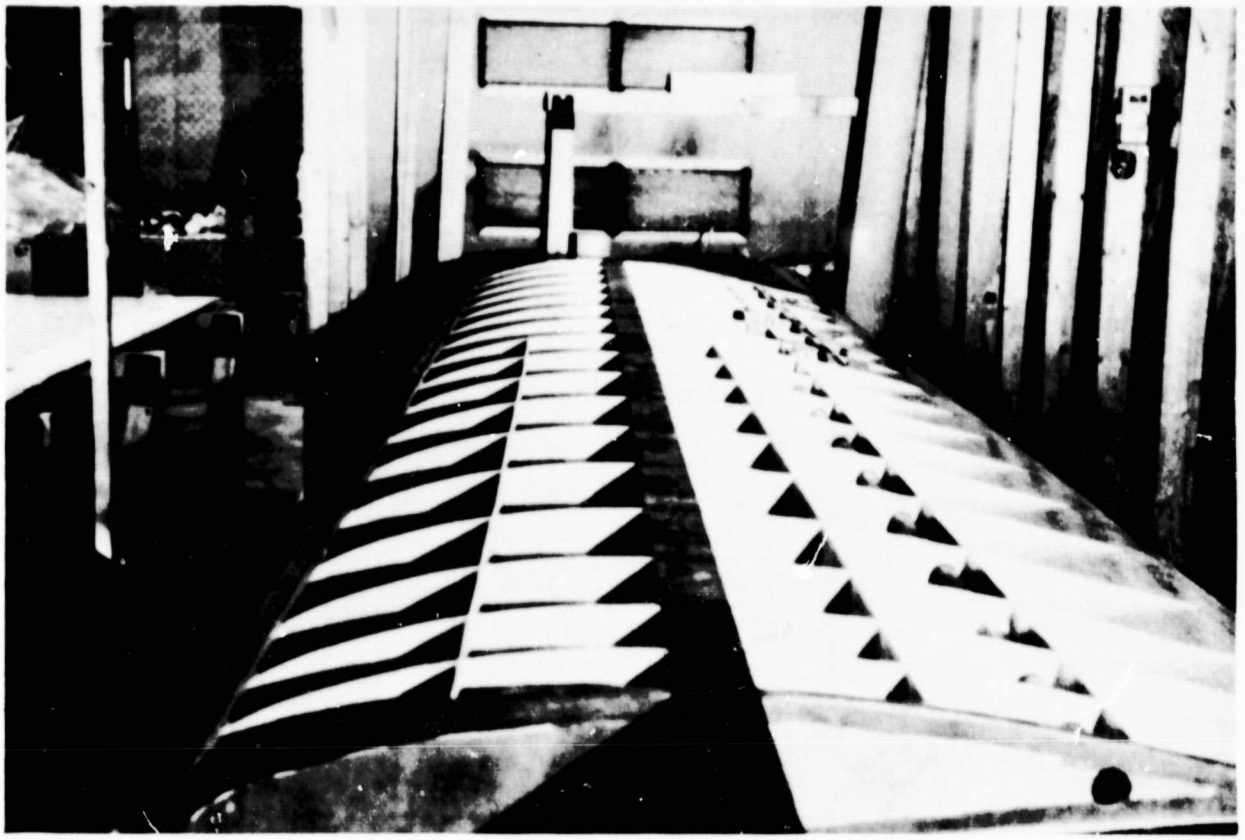

Figure 20 Semi-Span Wing Substructure

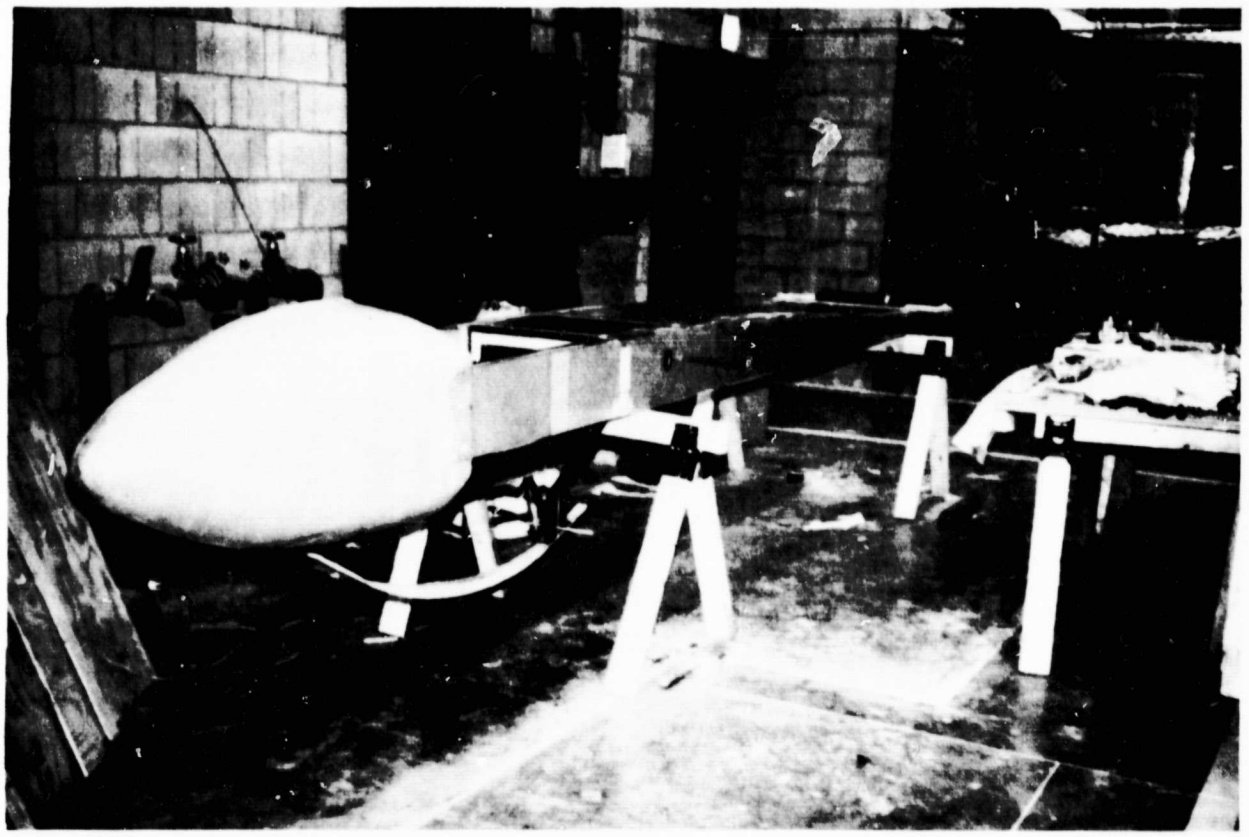

Figure 21 Fuselage

PART III

COMPAD (Computer Aided Design)

COMPAD (Computer Aided Design)
(L. J. Feeser and M. S. Shephard)

During this reporting period, emphasis within the computer aided design portion of the composites project has been put on enhancing RPI's finite element capabilities. This work is primarily concerned with three activities: (1) extension and maintenance of the finite element analysis programs available on RPI's computer systems, (2) initial development of a highly interactive finite element preprocessor and (3) linking the finite element analysis program, SPAR, to an array processor.

1. Finite Element Analysis Programs

Work has begun on the development of a new in-house finite element analysis program. This work is being carried out primarily as a series of term projects by a few selected students in RPI's finite element courses. This new program is being developed in a highly modular form so that new capabilities can be added with a minimum of effort.

Several other finite element method analysis programs are available to us; in fact, enhancement of RPI's finite element analysis capability has been accomplished mainly by the acquisition of additional finite element analysis codes. Table XI lists the finite element programs currently available along with a brief description of their capabilities. Nevertheless, we anticipate that at some point in the future

TABLE XI

LIST OF FINITE ELEMENT CODES AVAILABLE ON RPI'S COMPUTER SYSTEMS

Program	Computer	Capability
SPAR	PRIME	Static and dynamic analysis of both linear and nonlinear structural systems. Especially well suited for composites.
SAP IV	IBM, PRIME	Static and dynamic analysis of linear three-dimensional structural systems.
NONSAP	IBM	Same as SAP IV but with nonlinear capabilities. Nonlinearities may be due to large displacements, large strains and nonlinear material behavior.
ASHSD2	IBM	Evaluates the time dependent displacements and stresses of complex axisymmetric structures subjected to any arbitrary static or dynamic loading or base accelerations.
STRUDL	IBM	Static and dynamic analysis of linear structural system.
ANSYS*	PRIME	A wide variety of capabilities are available in this program including: a) static and dynamic analysis of linear and nonlinear systems (elastic, plastic, creep, swelling and large deflections handled), b) steady-state or transient heat transfer analysis (conduction, convection and radiation) and c) some fluid and electrical capabilities.

*By contract the use of ANSYS is limited to "small" problems for course work and student projects. It will not be available until Fall '79.

we will need to develop some new, then unavailable capabilites, and it will be far more efficient to add these capabilites to a general program that we know intimately, than it would be to modify one of the other existing programs or to write a complete program. An additional enhancement which will be discussed in conjunction with the array processor work is the creation of a version of SPAR that will run on a PDP 11/40 minicomputer.

2. Preprocessor Development

The finite element preprocessor currently under development will handle virtually all possible two-dimensional topologies. Extensive use of graphical input techniques and a unified overall design will result in a preprocessor that is both efficient and simple to use.

The development of a finite element model using a general preprocessing capability can be thought of as a three stage process. The first and most general phase is defining and discretizing the problem geometry. The second phase is defining problem-specific attributes such as material properties, boundary conditions and loads. The third phase is linking the preprocessor with the particular analysis program selected to solve the model. With this approach, only one general program for defining and discretizing problem geometry is required, since this process is the same for all finite element models. This program can then be linked to

one attribute editor for each class of problem to be considered. For example, one attribute editor may be used for stress analysis problems, another for heat transfer analysis and a third for fluid flow calculations. The last stage, the link to an analysis routine, is little more than a simple reformatting program; it is the only portion of the preprocessor program that will have to be repeated for each new analysis routine considered.

A two-dimensional preprocessor has been developed to the point that basic problem geometries can be defined and element meshes can be generated using a set of mesh generating capabilities. The operation of the preprocessor will be demonstrated in terms of a simple example.

The first step is the definition of a background planning grid which can be thought of as a piece of electronic graph paper. This planning grid is used later to obtain numerically exact input with interactive input devices by "hit testing" on the intersection of grid lines. In addition to defining and scaling a basic rectangular grid, interactive features allow the user to add and delete additional vertical and horizontal grid lines at user-specified levels and to move the origin to any grid intersection to produce a final planning grid such as the one shown in Figure 22.

The second step is to define the subregion boundary curves to be used by the mesh generators. Curves are defined interactively by first selecting the type of curve to be

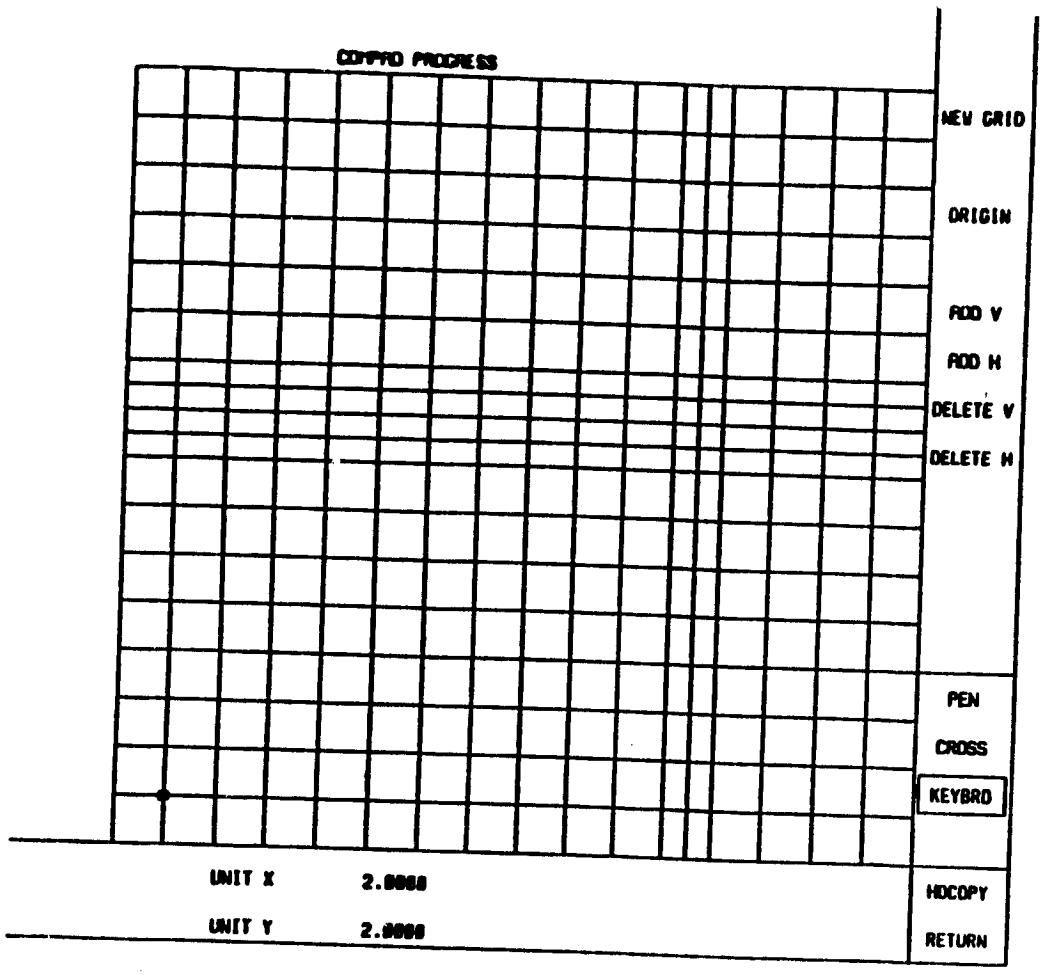

Figure 22

Background Planning Grid

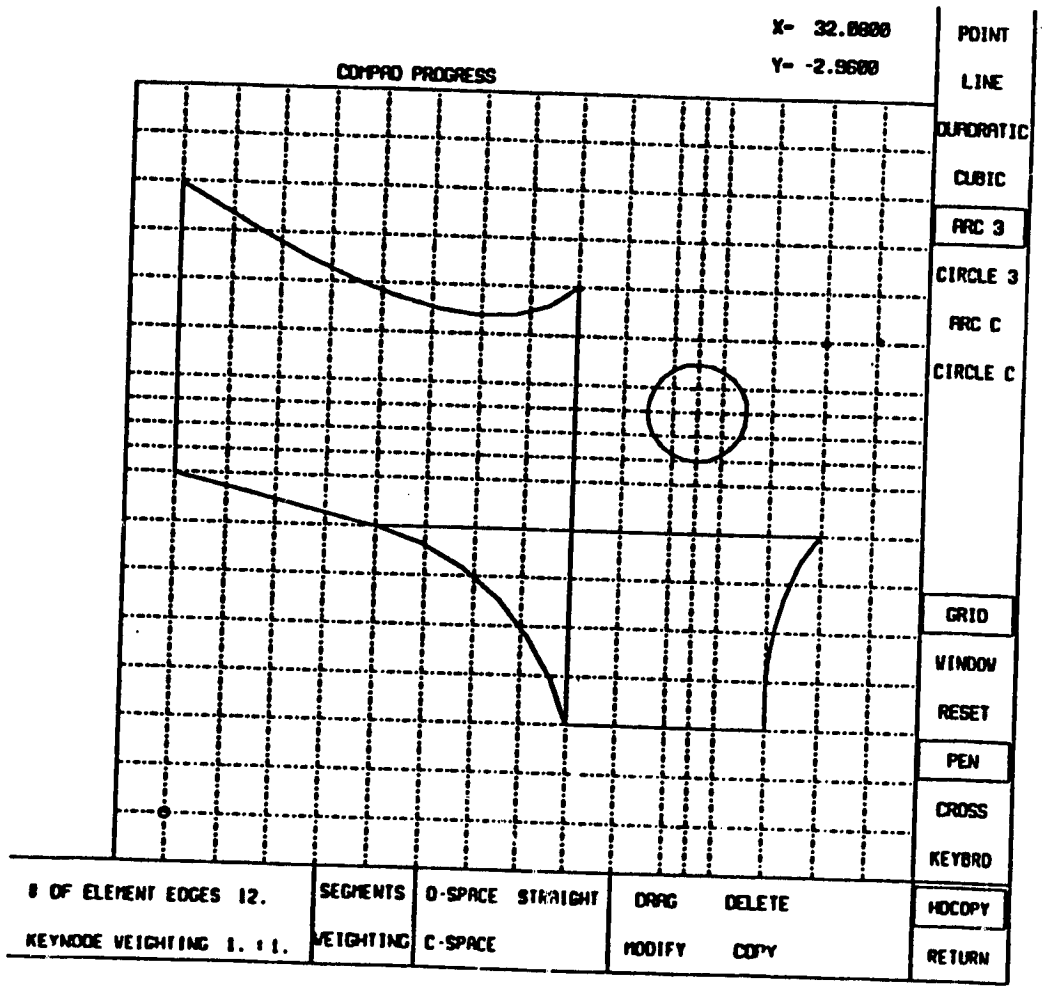

Figure 23

Boundary Curve Input

generated and then inputting the appropriate number of "key points" (either by use of the light pen, thumb wheels or keyboard) along the curve. The curve-generating options include single points, lines, circles, circular arcs and second and third degree polynomials computed by Lagrangian interpolation. A specified number of "key nodes" are then placed along the curve. The key nodes are the nodal location used by the mesh generator to define the resulting mesh. Since the number and location of the key nodes define the resulting mesh, options are available to specify both the number of key nodes to be placed on a curve and also a weighting parameter that forces the nodal spacings to vary from uniform along the length of the curve to being biased toward either end. Figure 23 shows the interactive input of a circular arc by three points along the arc while Figure 24 shows the final set of subregion boundary curves for the example problem.

After the subregion boundary curves have been defined, the geometry of the object has been determined and the element mesh can be generated. The element mesh is generated one subregion at a time by employing one of several available mesh generators.

Currently, three mesh generators have been implemented. The generators are computationally efficient and will produce well-conditioned grids in highly distorted regions. Each generator is based on a mathematical mapping that defines

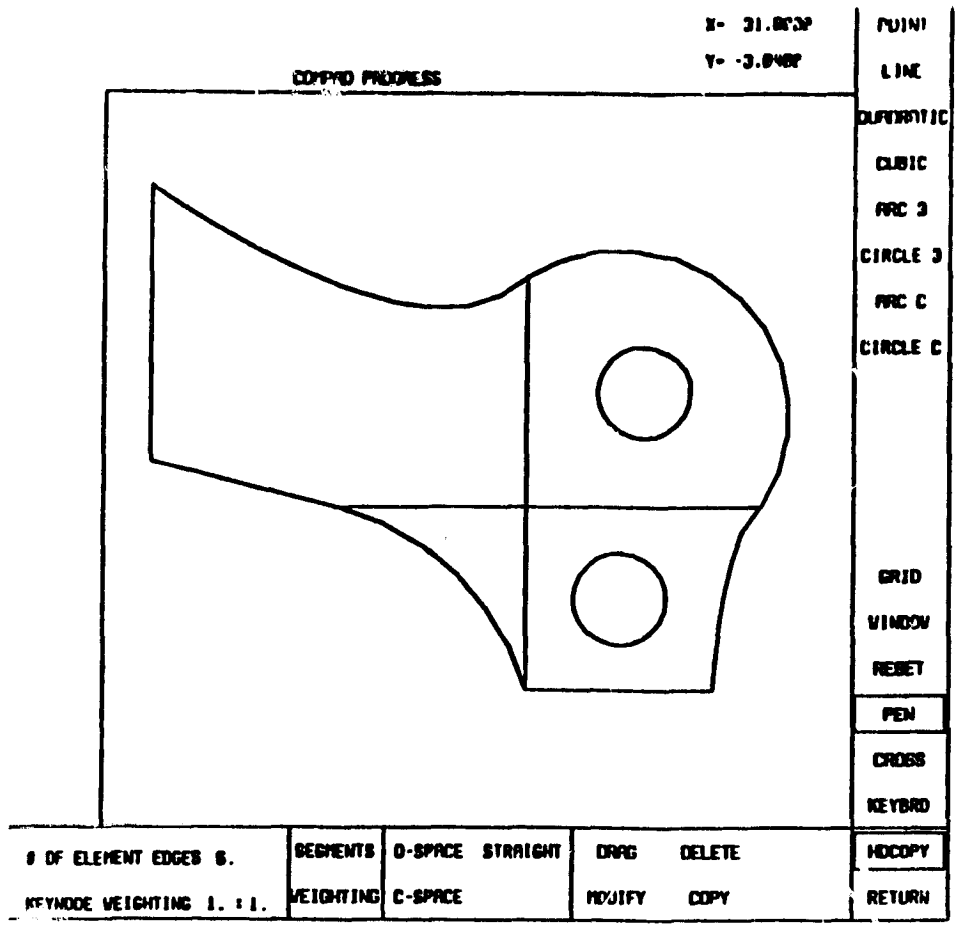

Figure 24

Final Curves

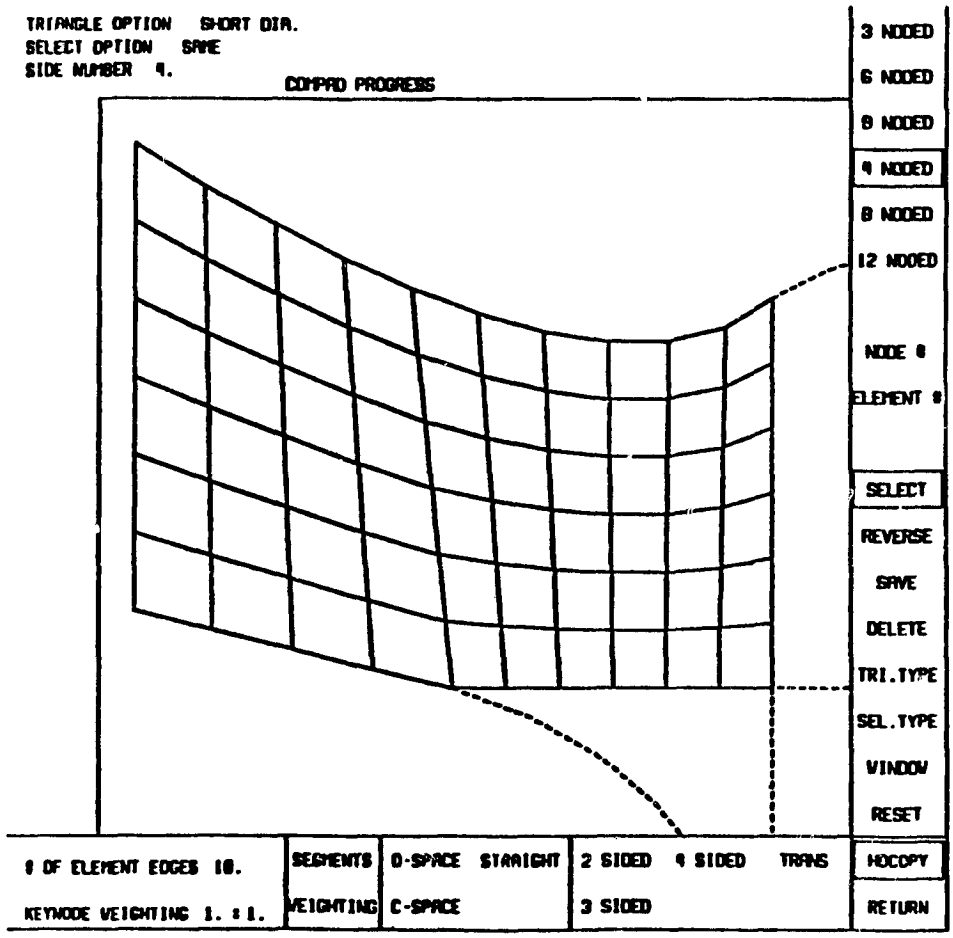

Figure 25

Four-Sided Mesh of Four-Noded Elements

internal node points in terms of the appropriate boundary key nodes by linear blending interpolants in one, two or three directions*. After the locations of the internal nodes have been defined, elements can be specified by appropriately connecting the nodes.

The mesh generators are invoked by first interactively indicating the subregion boundary curves that define the sides of a subregion, selecting an element type and then indicating the mesh generator to be used. Considering the left hand subregion of the example problem, the user indicates that the first three sides are one curve each, while the fourth side (the bottom of the subregion) is the concatenation of two curves. The user then indicates that he wants a four-sided subregion generated by the linear blending functions using four noded quadrilateral elements to define the mesh. The resulting mesh is shown in Figure 25 where a zoom feature has been used to look more closely at that subregion. Triangular elements can also be generated as shown in Figure 26. Figure 27 shows triangular elements generated in a three-sided region.

The upper right hand portion can be generated as a single subregion by mapping, via the linear blending functions, from

---

*Haber, R. B., M. S. Shephard, J. F. Abel, R. H. Gallagher and D. P. Greenberg, "A Generalized Graphic Preprocessor for Two-Dimensional Finite Element Analysis", Computer Graphics a quarterly report of SIGGRAPH-ACM, Vol. 12, No. 3, August 1978, pp. 323-329.

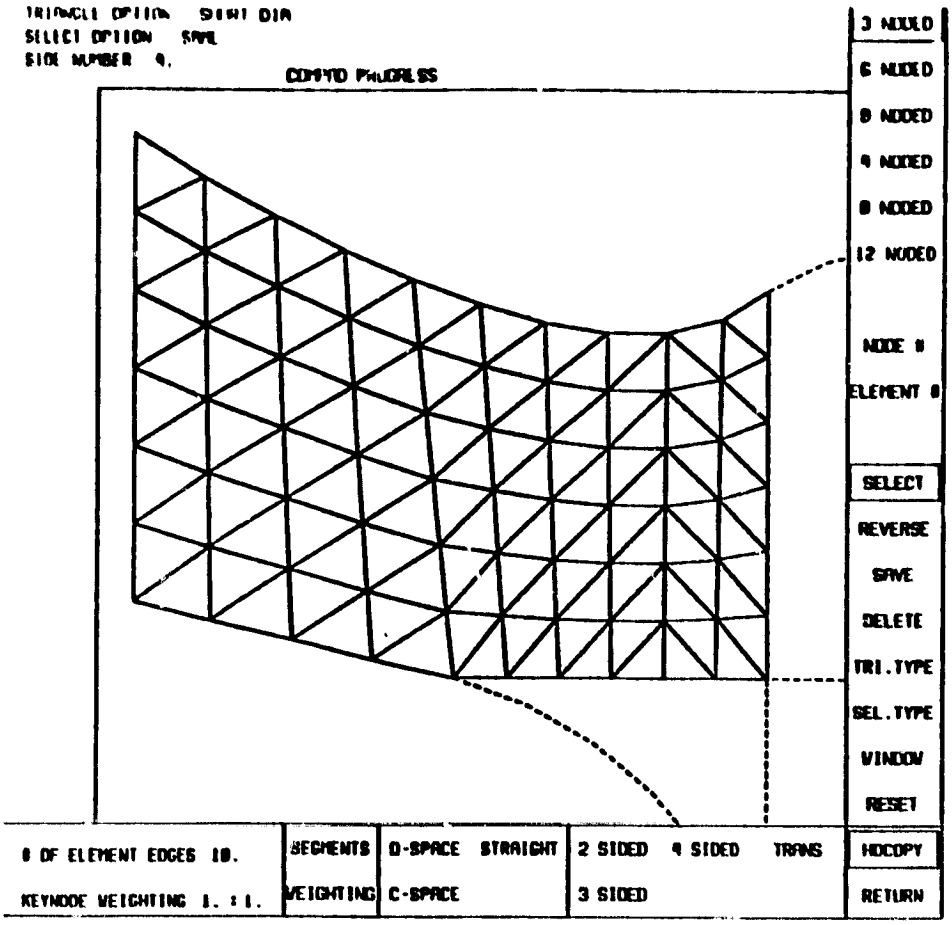

Figure 26

Four-Sided Mesh for Three-Noded Elements

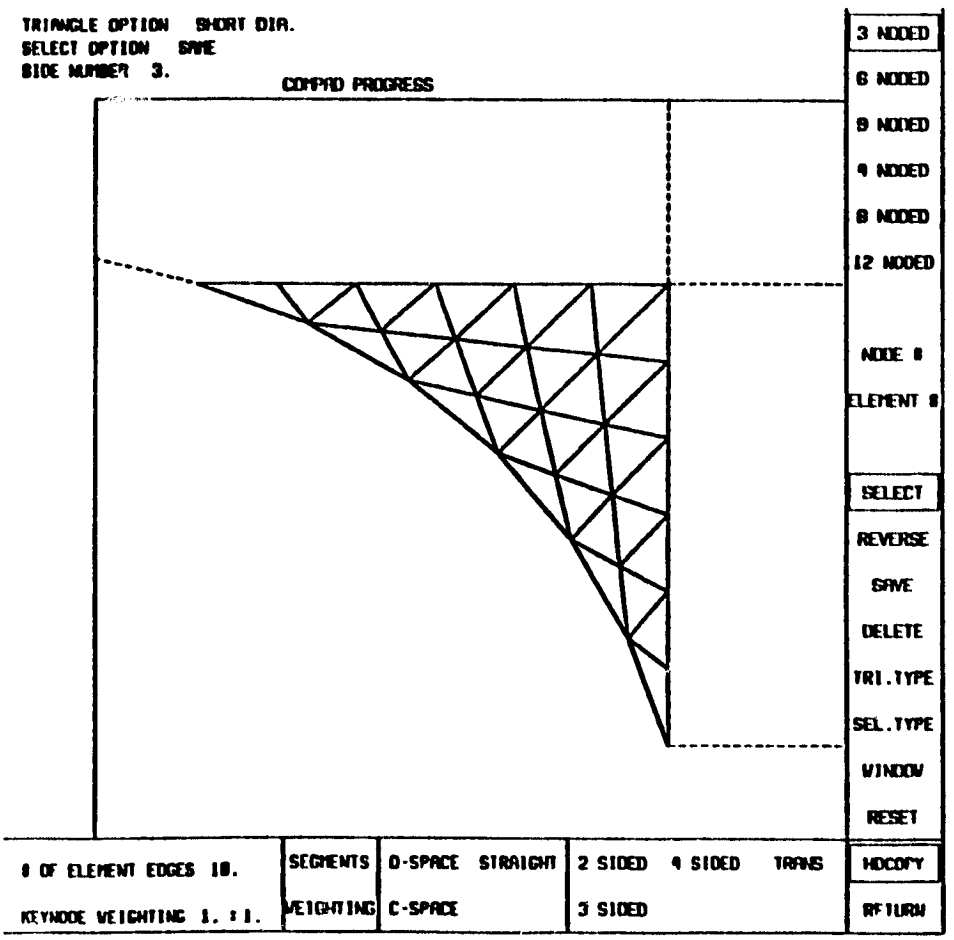

Figure 27

Three-Sided Mesh of Three-Noded Elements

the circle defining the hole to the three curves defining the outside of the subregion. Figure 28 shows a four element deep mesh, biased towards the hole, generated in this manner. Figure 29 shows the completed mesh for the example problem.

3. Array Processor for SPAR

As discussed in the last semi-annual progress report, preliminary feasibility studies have indicated the potential benefits of using an array processor in conjunction with the SPAR finite element analysis program. Work is currently under way to link SPAR with a Floating Point Systems AP120 array processor. Since this array processor is operated from a PDP 11/40 mini-computer, effort has concentrated on creating a modified version of SPAR to run on the 11/40. As this work is being conducted, areas of code where an array processor may be used are being identified and considered as candidates for replacement by array processor operations.

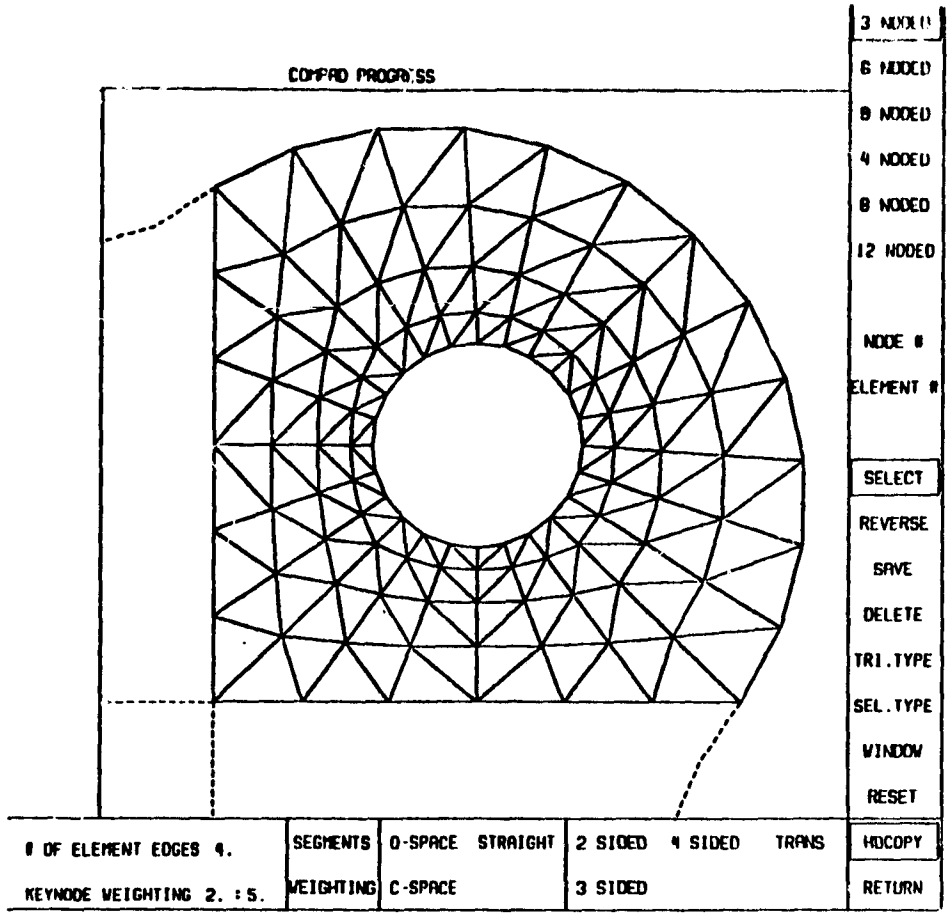

Figure 28

Two-Sided Mesh of Three-Noded Elements

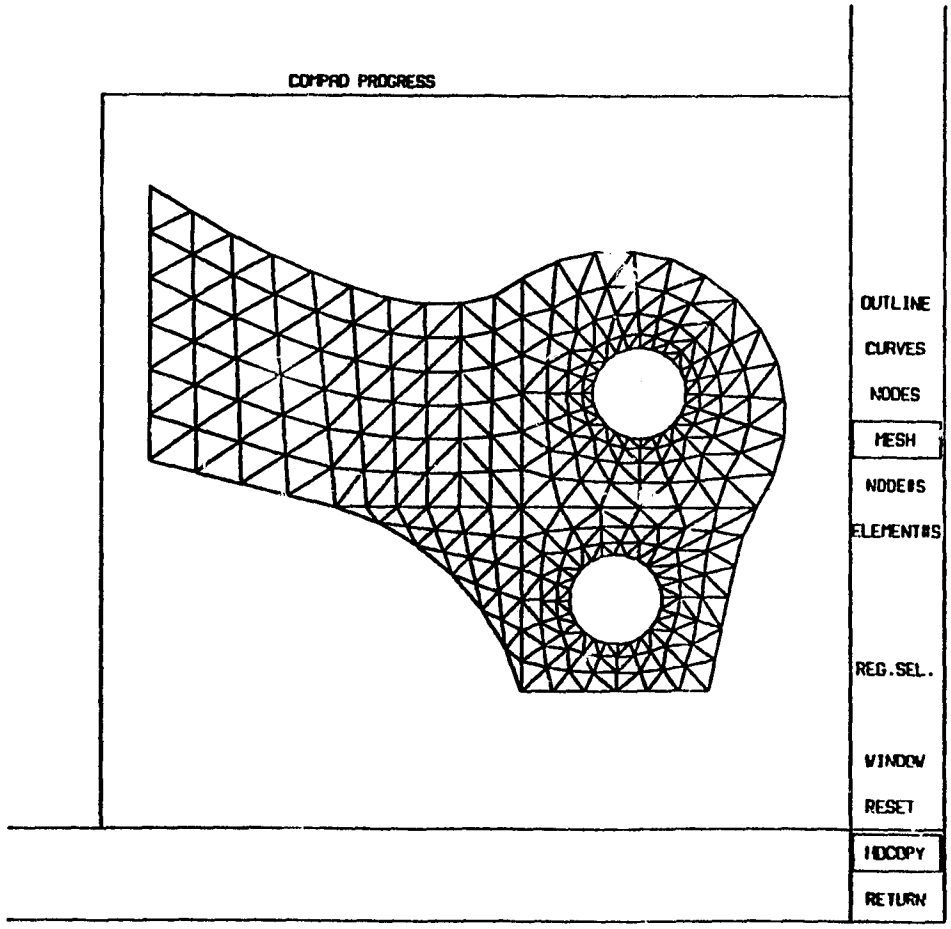

Figure 29

Final Mesh

PART IV

INSURE (Innovative and Supporting Research)

Progress on composites research is reported in the individual write-ups on the succeeding pages in the following areas:

Advanced Analysis Methods for Composite Structures

Ultrasonic Non-Destructive Testing Developments

Physical Properties of Epoxy Resins and Composites

Fatigue in Composite Materials

Transverse Thermal Expansion of Carbon/Epoxy Composites

ADVANCED ANALYSIS METHODS FOR COMPOSITE STRUCTURES

Senior Investigator: E. J. Brunelle

During the reporting period three diverse areas of research were undertaken. The first two areas appear to be relatively short term ventures even though one of them has become diffuse enough to lead to a number of sub-areas that are each producing interesting results. The third area is a more ambitious undertaking and is considered to be a longer term effort with potentially promising and useful results. Interestingly enough, research in the first two areas was initiated only after assuming that the results should have been in the literature; however no trace of them was found, and it was, therefore, deemed worthwhile to spend some time filling in the theoretical gaps.

The first area of research delineates the laws governing the variation of the properties of an orthotropic lamina, of an anisotropic lamina and of a laminate comprised of orthotropic laminas with changes in the orientation of the coordinate axes. A nondimensional number $B = \frac{U_2}{4U_3}$ completely governs these rotational properties of an orthotropic lamina and depending on whether $B>1$ or $B<1$, "regular" or "anomalous" rotational properties are observed. This is not simply an "academic" issue since typical values of B for boron/epoxy, graphite/epoxy and glass/epoxy are .99, 1.01 and 1.3 respectively. Besides obtaining detailed rotational information on the $\bar{Q}_{ij}$ (elements of the reduced stiffness matrix in the

transformed stress-strain relation) as influenced by B, a simple inequality has been derived that identifies a new composite material as being "regular" or "anomalous". This inequality (see Figure 30) should be of particular interest to the physical chemists/materials engineers who are involved with developing new fibrous composite materials.

The second area of research traces its origins to a desire to reduce the number of elastic constants in any given problem to a smaller number of "cluster constants" which can be used more efficiently in parameter studies of any given problem. For example, if a problem involving four elastic constants could be reduced to a problem involving only one "cluster constant", physical insight into the problem becomes much clearer, more general solutions are usually possible. Furthermore, what was originally an enormous computational effort (Note that for a parametric study of the above cited generic problem, sufficient sets and combinations of the four constants must be considered.) can be reduced to a one parameter family of solutions.

"Cluster constants" have been derived by employing affine transformations on the dependent variables as well as the independent variables. This method has been quite successful and has produced some diverse results which follow:

1) A composite shell problem that was posed, but not solved correctly, almost two decades ago in a classic paper by Pister, Dong and Taylor is now easily solved.

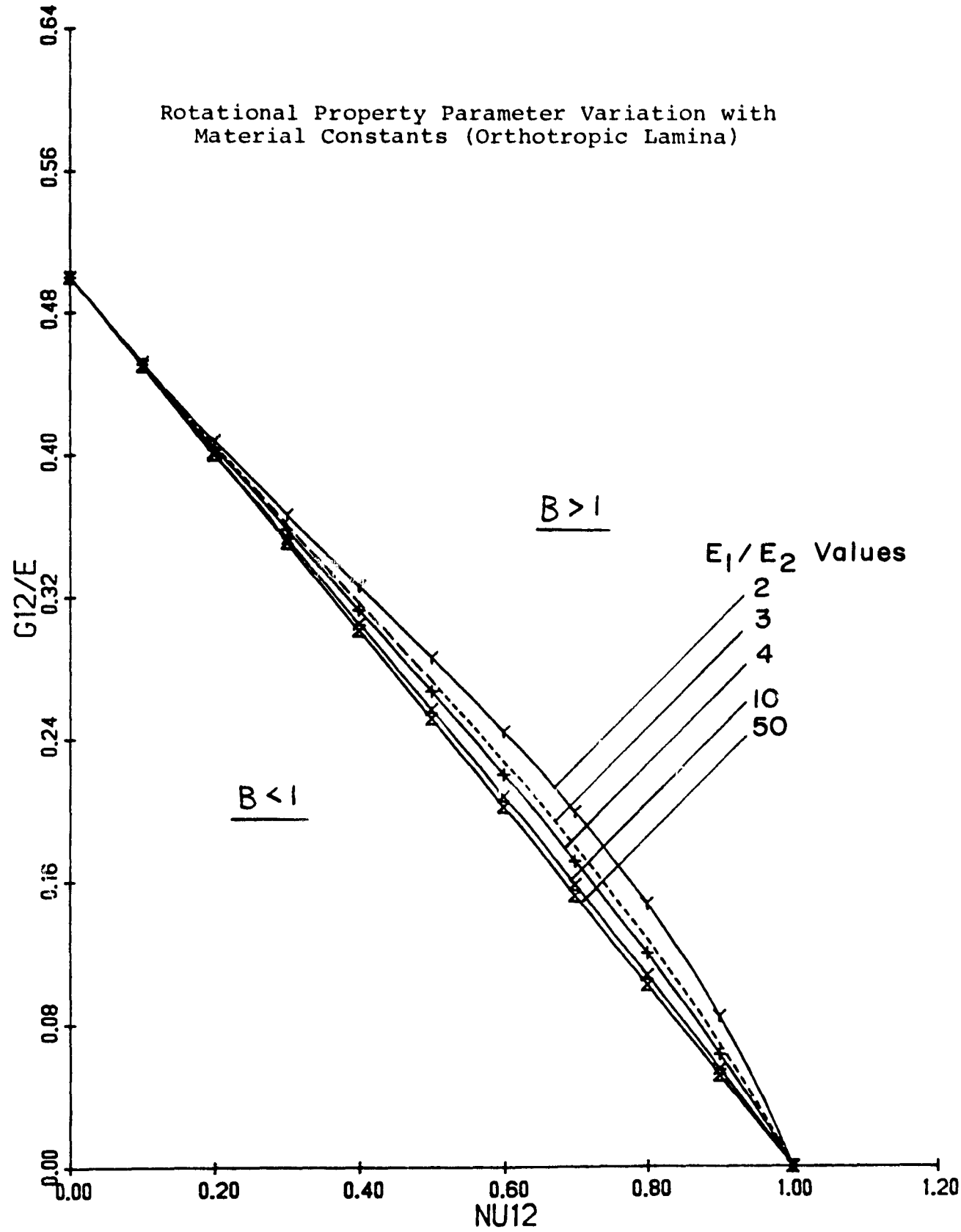
Rotational Property Parameter Variation with
Material Constants (Orthotropic Lamina)
G12/E
NU12
0.00
0.08
0.16
0.24
0.32
0.40
0.48
0.56
0.64
0.00
0.20
0.40
0.60
0.80
1.00
1.20
B > 1
B < 1
E1 / E2 Values
2
3
4
10
50

Figure 30

2) The dependence of shear deformation effects on boundary conditions has been shown dramatically by a general solution to a composite plate strip problem. The result, which is well documented in earlier work for (simpler) transversely isotropic beams and plates, is that the effects of shear deformation are exacerbated by any form of increased boundary restraint; obviously this is not the trend one would prefer to see.

3) The specially orthotropic plate, which provides important bounds for composite plate problems (upper bounds for buckling, etc.), can be reduced to a one parameter family of solutions. Master curves can thus be presented for any and all static, dynamic and instability problems associated with the specially orthotropic plate.

The third area of research seeks a systematic method of generating hierachies of (elastic) composite beam, plate and shell equations that govern the static, dynamic and stability behavior of realistic composite materials structures. In this development, a proper accounting is to be made of (i) conservative and non-conservative arbitrary initial stress states, (ii) the accompanying initial displacement gradient field [this has been almost completely neglected in the literature of even single layer structures] and (iii) arbitrary states of initial [stress-free] displacements so that the effects of "imperfection sensitivity" are an integral part of the formulation.

The progenitor of this method, as developed by the present investigator, will reproduce all the standard results of structural mechanics (with some interesting addtional features) when the simplest possible displacement assumptions of the hierachy are introduced into a non-classical virtual work theorem. The results of this research should be considered as a serious candidate to provide the basic equations to be used in the next generation of finite element programs for routine structural analysis. It may be desireable to give these finite element method (FEM) programs self-diagnostic capability such that the programs evaluate the input and automatically select the proper hierachy of equations that will most properly and most economically solve the given structural problem. In other words, the self-diagnostic capability should be designed to prevent "overkill" or "underkill" in the solution of any given problem.

ULTRASONIC NON-DESTRUCTIVE TESTING DEVELOPMENTS

Senior Investigators: H. F. Tiersten
P. K. Das

Since the last report was submitted, trapped energy mode focusing transducers have been fabricated by plating a number of concentric rings on a PZT-7A plate. The concentric ring structure acts as a Fresnel lens and focuses the ultrasonic waves. Two transducers, operating in the frequency range centered at 2.5MHz, have been fabricated. The first order diffraction pattern from a laser probe is being used to study the radiation pattern in water at various distances from the transducer. From the near field radiation pattern it has been confirmed that the acoustic isolation between the rings is excellent.

A doubly focused acoustic imaging system, which incorporates focusing transducers at both the transmitting and receiving ends, is being used for imaging of composite materials. Scanning is performed using a Z-80 microprocessing system which also stores and displays the image. Images of the ultrasonic transmission through composite materials, which were prepared for tensile testing, are being obtained (See Part I, CAPCOMP, section 4). Preliminary results compare well with those obtained using other testing procedures and reveal certain features which have never been observed by means of non-destructive testing procedures.

The analysis of mode coupling in thickness-extensional trapped energy mode transducers with strip electrodes has been completed. The frequency spectra occur in closed loops due to the large coupling in PZT-7A. The analysis uncovered modes with numerous peaks and valleys across the electrode in the strongly coupled regions. The lowest complex dispersion curves for PZT-7A plates have been determined and will be employed in the analysis of energy trapping in the lower frequency range, which has been observed experimentally. An analysis of PZT-7A plates driven into thickness-extensional trapped energy vibrations by the application of a voltage across strip electrodes is being performed. The plate waves in the unelectroded region that carry energy away from the trapped mode are being included in the treatment. All previous treatments were limited to the consideration of an eigenvalue problem; the current effort will enable consideration of the inhomogeneous forced vibration problem.

PHYSICAL PROPERTIES OF EPOXY RESINS AND COMPOSITES

Senior Investigator: S. S. Sternstein

This project is concerned with the mechanical characterization of epoxy neat resins, including particularly the effects of moisture, temperature and stress histories and ultimately the dependence of the properties of high performance composites on neat resin behavior.

The first phase of this work has involved the application of inhomogeneous swelling theory developed previously for filled elastomer systems to the water swelling of a neat resin containing isolated carbon fibers. A principal problem area has been the development of a suitable consitutive equation for describing the thermodynamic interactions of water with neat resin and the subsequent mechanical properties of the swollen resin. Extensive data from the literature have been used to develop a model constitutive equation. Such an equation has now been formulated, and it appears to fit the available data. Briefly, the model employs a standard lattice model calculation for the combinatorial entropy of mixing and a concentration-dependent Flory-Huggins parameter for the excess free energy of mixing.

The mechanical work function required for the inhomogeneous swelling field problem has been developed from the Gaussian theory of rubber elasticity and utilizes a concentration-dependent crosslink density. In effect, this allows

the modulus to depend explicitly on water concentration. This is to be contrasted with the usual treatment of rubber swelling in which modulus and crosslink density do not depend explicitly on concentration but rather implicitly through the volumetric swelling ratio (a simple dilution calculation). It is not suggested that the revised Gaussian model has any particular molecular significance; however, it fits the data well. One can conjecture that the model is that of a two-crosslink density network, one being due to the true chemical crosslinks in the epoxy resin and the other a physical crosslink network, e.g., due to hydrogen bonds. It is the latter network which is destroyed by water absorption and results in reduced modulus.

The inhomogeneous swelling theory has been revised for application to cylindrical inclusions, e.g., carbon fibers and sample calculations have been performed using the new constitutive equations. It is found that the overall swelling ratio of the epoxy is little affected by the presence of a carbon fiber. However, the local stresses and strains in the vicinity of the interface (between the fiber and epoxy matrix) are strongly influenced. Thus, a global view of swelling in composites, e.g., by weight gain studies, would appear as a simple reduction of water absorption in proportion to the fiber content. However, a local view leads to a much deeper insight into the role which water absorption plays. For example, it is found that the radial stress at

the fiber interface generated by inhomogeneous swelling can be as high as 50% of the epoxy tensile strength.

The calculations have also shown that under appropriate conditions determined by the constitutive parameters the water concentration at the interface is higher than at further distance into the matrix. This is in sharp contrast to swelling in a filled rubber where the swelling at the interface is markedly reduced.

Additional calculations on swelling instability (e.g., void formation) are in progress. A publication on the swelling field calculations is being prepared.

The second phase of this work involves the dynamic mechanical characterization of swollen neat resins. Briefly, the water-equilibrated samples are being subjected to rapid temperature scans and the dynamic mechanical loss factor is being obtained at frequencies from 1 Hz to 100 Hz. These data will be required for further analysis of the water swelling of epoxy resins.

FATIGUE IN COMPOSITE MATERIALS

Senior Investigators: E. Krempl

During this reporting period activities were mostly devoted to the design of a biaxial fatigue test specimen and associated fixtures. The Cyclic Strain Laboratory is equipped with an MTS tension-torsion hydraulic test system, and we plan to utilize this testing machine in our experiments. Much thought has been given to means by which we can insure that specimens will not fail at the mounting grips when tested with this equipment.

The proposed specimen is shown in Figure 31. It is made by wrapping graphite-epoxy tape at ±45° around an aluminum mandrel. At present four layers of tape are used. At each end, 90° layers are built up and subsequently machined to the taper shown in Figure 31.

The specimen is made to fit into the fixture shown in Figure 32. The fixture includes a circular main part (1) which bolts to the testing machine crosshead. A circular cover plate (2) wedges the specimen into the main part through the circular plug (3) with square ends which fits into a corresponding opening in the main part (1) and by the split wedge (5) and the ring wedge (4).

The specimen is mounted by tightening the bolts on the circular cover plate (2). Then hydraulic pressure is admitted through a separate part which pressurizes the plug

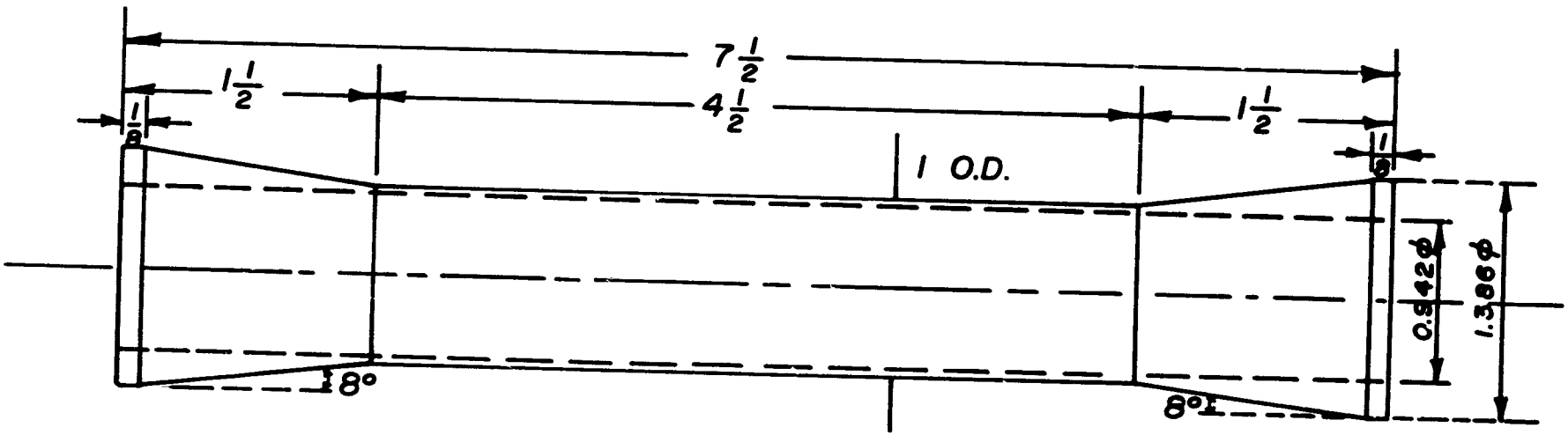

Unit: Inch
Scale: 1/1

Graphite/Epoxy Thin-Walled Tube Specimen for Bi-Axial Fatigue Testing
Wrap-Around Technique of 4 Layers ±45° Graphite/Epoxy

Figure 31

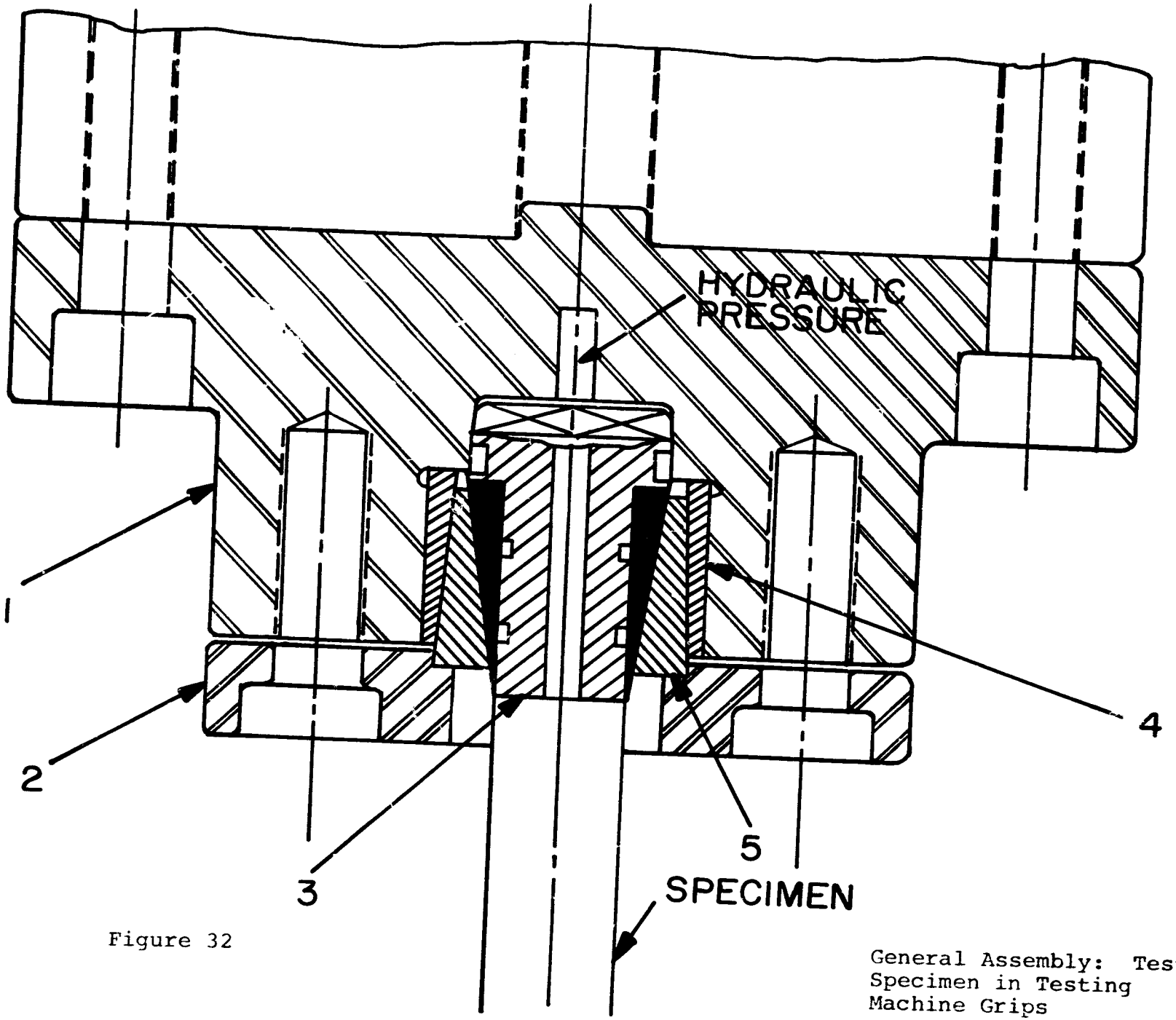

Figure 32

General Assembly: Test Specimen in Testing Machine Grips

and keeps the wedge assembly under constant pressure. It prevents the loosening of the fit due to relaxation in the specimen.

The axial force is transmitted through the wedges. Torque transmission relies entirely on friction between the plug (13) and the specimen and the split wedge (5) and the specimen.

The plug (3) has a central bore which can be drilled through the square ends. This bore will permit the addition of internal pressure as an independent load system in addition to the axial loading and the torque presently planned.

Prototype test specimens have been made with no difficulty, and machining of the fixture is nearing completion. Preliminary tests are planned with the MTS tension-torsion system in the next reporting period.

In parallel with the design and fabrication work described above, uniaxial fatigue tests on $\{0/\pm 45_2/90\}2s$ and $\{90/\mp 45_2/0\}2s$ graphite epoxy 12-ply laminates as reported during the last period continued, with special consideration of frequency effects.

TRANSVERSE THERMAL EXPANSION OF CARBON FIBER/EPOXY COMPOSITES

Senior Investigators: R. J. Diefendorf
C. LeMaistre

It is important to be able to predict physical properties of laminates from constituent properties by means of micromechanical analysis. Several authors have developed micromechanical theories and have been able to obtain reasonable correlation with experimental data. This is particularly true of elastic and thermal properties with isotropic constituents[1-5]*. Moreover, the longitudinal TCE, $\hat{\alpha}_{11}$, derived by Greszczuk[6] and Schapery[7] is even effective for composite systems which have anisotropic fibers (graphite/epoxy). Their expression for $\hat{\alpha}_{11}$ is:

$$\hat{\alpha}_{11} = \frac{\alpha_m V_m E_m + \alpha_f V_f E_f}{E_m(1 - V_f) + E_f V_f} \qquad (1)$$

where α, V, E stand for TCE, volume ratio and Young's modulus; and m and f subscripts stand for matrix and fiber, respectively. This equation assumes that Poisson's ratio of the fiber and matrix are equal. The good agreement is obtained because the fiber properties dominate in the 0° orientation, and fiber properties are measured parallel to the fiber axis.

Prediction formulas for transverse TCE do not fare as well for graphite reinforced composites as they do for other composites due to the anisotropy of the fibers. The theories

---

*Nos. in raised parentheses refer to the References listed on pages 98 and 99.

to be presented in the following paragraphs make the following basic assumptions:

1) The ply is macroscopically homogeneous, linearly elastic and generally orthotropic.
2) The fibers and matrix are linearly elastic, homogeneous and isotropic.
3) There is complete bonding at the interface of the constituents, and there is no transition region between them.
4) The ply is initially in a stress-free state.
5) The fibers are regularly spaced and aligned.[8]

A mechanics of materials approach was used by Greszczuk[6] to determine $\hat{\alpha}_{11}$ and $\hat{\alpha}_{22}$. The quantity $\hat{\alpha}_{11}$ was presented in Equation 1 and $\hat{\alpha}_{22}$ is expressed as follows:

$$\hat{\alpha}_{22} = \frac{1}{E_2}[\alpha_o E_o \beta + \alpha_m E_m (1 - \beta)] \tag{2}$$

$$\alpha_o = \alpha_m(1 - 2\beta) + 2\alpha_f\beta - \nu_m(\alpha_f - \alpha_m)(1 - 2\beta) \tag{3}$$

$$E_o = \frac{E_m E_f}{[E_f(1 - 2\beta) + 2E_m\beta]} \tag{4}$$

$$\hat{E}_2 = E_o\beta + E_m(1 - \beta) \tag{5}$$

$$\beta = \sqrt{\frac{V_f}{\pi}} \tag{6}$$

This formula assumes circular filaments. Schapery[7] developed bounds on the TCE of isotropic constituent composites by employing extremum principles of thermoelasticity. As shown before, Equation 1, Schapery's formula for $\hat{\alpha}_{11}$ is the same as that derived by Greszczuk. Schapery also presents a simple

expression as an upper bound for $\hat{\alpha}_{22}$ derived by Wang Fo-Fe[9]:

$$\hat{\alpha}_{22} = (1 + \nu_m)\alpha_m V_m + (1 + \nu_f)\alpha_f V_f - \hat{\alpha}_{11}[\nu_f V_f + \nu_m V_m] \quad (7)$$

The results from formula (7) compare well with experimental results from fiber glass composites.

Fahmy and Ragia-Ellozy[10] and Kahn[11] applied finite element analysis to determine $\hat{\alpha}_{11}$ and $\hat{\alpha}_{22}$ for a lamina. This approach provides a rigorous solution for $\hat{\alpha}_{22}$, but requires a sophisticated microstructural analysis of the composite system and does not provide a readily accessible equation for determining $\hat{\alpha}_{22}$ from constituent properties. Kahn also develops an equation for $\hat{\alpha}_{22}$, treating the fiber as a solid rod of radius 'a' and the matrix as a tube of inner radius 'a' and outer radius 'b'. The matrix tube is subjected to an internal pressure, P, whose sign depends on the thermal mismatch between fiber and matrix:

$$\hat{\alpha}_{22} = \alpha_m + \frac{(\varepsilon_{\theta m})_b}{\Delta T} \quad (8)$$

$$(\varepsilon_{\theta m})_b = \frac{1}{E_m}\left[\frac{2P\chi}{1 - \chi} - \nu_m \sigma_{zm}\right] \quad (9)$$

$$\sigma_{z_m} = P\left[1 + \frac{E_f(1 - \nu_m)}{E_m(1 - V_f)(1 + \nu_f) + E_f V_f(1 + \nu_m)}\right]\frac{V_f}{1 - V_f} \quad (10)$$

These equations result in a curve which falls between the rule of mixture lower bound solution and Schapery's upper bound equation. Finally, Levin[12] provides an anisotropic analysis for the thermal expansion coefficients. No comparison is made to experimental results for almost all analyses.

In an attempt to evaluate the applicability of these theories, thermal expansion specimens were fabricated and tested on a push-rod dilatometer. The material selected for this investigation was the Fiberite 1048 AE graphite/epoxy system. Components consist of Union Carbide T-300 graphite fiber and Fiberite's 121°C (250°F) 48A resin in prepreg form. Test specimens were fabricated on a Dake 75-ton press with 19" x 19" programmable heated platens. The cure cycles were programmed with a Data Trac and fully monitored. Nine specimens, 6" x 6", were fabricated with varying fiber volume, from which five expansion samples, 2" long, approximately 1/2" in highth and thickness varying depending on fiber volume, were cut. All nine specimens contained 32 plies unidirectional prepreg cured at various pressures, quantity of bleeders and excess resin to achieve the required resin content. Neat resin was cured in the same manner as the laminates under vacuum pressure to remove porosity. Similar dimensions were used for the resin TCE specimens. Dog-bone tensile specimens were fabricated for determination of tensile modulus and Poisson's ratio of the resin.

TCE specimens were conditioned in an air circulating oven at 110°C for 24 hours and stored in a desiccator until tested in an attempt to eliminate moisture induced variations in the thermal expansion measurement[12,13]. Specimens were weighed before and after testing to determine moisture loss during testing.

Thermal expansion measurements were performed on a modified Thermo-Physics Corporation push rod dilatometer. Samples were heated from room temperature to 100°C at a low rate of 0.75°C/min. to minimize discrepancies which may arise from the variation in thickness and thermal conductivity of the different fiber volume samples. The linear TCE was derived from a continuous recording of length, utilizing a precision LVDT, with resulting accuracy of 0.1×10^{-6}/°C.

Two methods were used to determine fiber volume; 1) visual count method using exploded photo-micrographs of the composite microstructure and 2) Boeing's MS8-212A nitric acid digestion method. Densities were determined utilizing ASTM D792 "Tests for specific gravity and density of plastics by displacement, Method A".

Mechanical testing was performed on an Instron screw-type universal testing machine at a crosshead rate of 0.005"/min., and strain data was recorded on a Data Logger. The 1048 AE composite's mechanical property data used were results of early testing by Kowalski[14].

The results of individual testing indicate that the 24 hour thermal conditioning of the TCE specimens was effective in minimizing the moisture response on expansion. The typical peaking, probably caused by the T_g depression, evident in past work [12,13,15] due to absorbed moisture, was not noted. Weight loss related to moisture desorption during testing was less than .03% in all samples tested.

Table XII shows average transverse TCE from 30°C to 100°C versus fiber volume. These results are plotted on Figure 33. From these data points, an estimate of $\hat{\alpha}_{22}$ for the individual fiber was calculated by utilizing a least-mean-squares extrapolation to V_f = 100%. It is noted that a modified rule of mixtures behavior is assumed and that a straight line is valid to approximate $\hat{\alpha}_{22}$. From this analysis it is estimated that $\hat{\alpha}_{22}$ for T-300 graphite fiber has a value of 8.8 x 10^{-6}/°C in a temperature range of 30°C - 100°C. This result is similar to a result obtained by Ishikawa[15] who estimates a value of 8.6 x 10^{-6}/°C. However, it is important to note that Ishikawa's method appears to be self-fulfilling in that $\hat{\alpha}_{22}$ is determined by extrapolating values from a theoretical curve and plugging the results back into the theory to prove its fit.

In order to correlate this estimated value of $\hat{\alpha}_{22}$ of T-300 to Schapery's upper bound solution, elastic constants of the matrix are required. Test results indicate that E_m = .55 x 10^6 psi and ν_m = .35. These values agree with typical values of E_m and for other epoxy resins used in composites[16].

The upper bound equation presented by Schapery was modified

$$\hat{\alpha}_{22} = (1 - \nu_m)\alpha_m V_m + (1 + \nu_{f_{12}})\alpha_{f_{22}} V_f - \hat{\alpha}_a(\nu_{f_{12}} V_f + \nu_m V_m) \quad (7a)$$

to include fiber anisotropy. $\hat{\alpha}_a$ is defined by Equation (1) and would appear to be close to the value $\hat{\alpha}_{f_{11}}$ for high modulus fibers at moderate or high volume fractions. Direct application of this equation gives a theoretical curve that is higher than all experimental values, because the boundary condition

TABLE XII

TEST RESULTS: TRANSVERSE TCE VERSUS FIBER VOLUME

Specimen Number	Density (g/cc)	V_f (nitric digest)	V_f (micro-photo)	TCE ($\times 10^{-6}$/°C) (ave.:30-100°C)
11	1.542	67.2		23.5
12	1.595	70.1		27.2
13	1.454	--		25.1
14	1.586	64.2		26.6
15	1.585	69.2		25.2
ave.		67.7	68.7	25.5
21	1.553	--		30.4
22	1.563	65.1		29.7
23	1.524	64.7		29.7
24	1.533	64.6		28.2
25	1.580	69.3		26.8
ave.		65.9	63.0	28.9
31	1.628	67.3		31.9
32	1.550	63.9		28.7
33	1.543	66.1		30.1
34	1.514	62.4		33.7
35	1.542	63.8		31.0
ave.		64.7	64.2	31.1
41	1.530	61.9		32.3
42	1.557	62.1		32.9
43	1.579	62.9		29.7
44	1.557	62.4		33.9
45	1.530	63.8		31.3
ave.		62.3	60.9	32.0
51	1.532	59.2		36.2
52	1.537	59.4		31.7
53	1.525	58.8		35.4
54	1.500	57.4		34.7
55	1.513	58.1		33.4
ave.		58.6	56.3	34.3

TABLE XII continued

Specimen Number	Density (g/cc)	V_f (nitric digest)	V_f (micro-photo)	TCE ($x10^{-6}$/°C) (ave.:30-100°C)
61	1.470	43.0		34.7
62	1.451	50.9		37.1
63	1.443	50.4		39.9
64	1.454	51.2		40.5
65	1.449	51.3		39.1
ave.		49.4	51.5	38.2
71	1.501	52.1		38.3
72	1.492	54.4		36.6
73	1.489	54.4		38.1
74	1.489	54.1		39.1
75	1.478	54.9		35.0
ave.		54.9	53.6	37.4
81	1.354	46.9		40.0
82	1.401	46.8		42.4
83	1.407	--		38.6
84	1.417	48.1		41.2
85	1.431	52.0		38.8
ave.		48.4	49.6	40.2
91	1.393	40.4		46.1
92	1.343	38.4		44.1
93	1.328	37.3		41.0
94	1.342	38.7		44.4
95	1.389	41.3		43.3
ave.		39.2	36.6	43.8
101	1.185			51.9
102	1.201			53.9
103	1.200	00.0		52.5
104	1.213			52.8
105	1.205			54.8
ave.				53.2

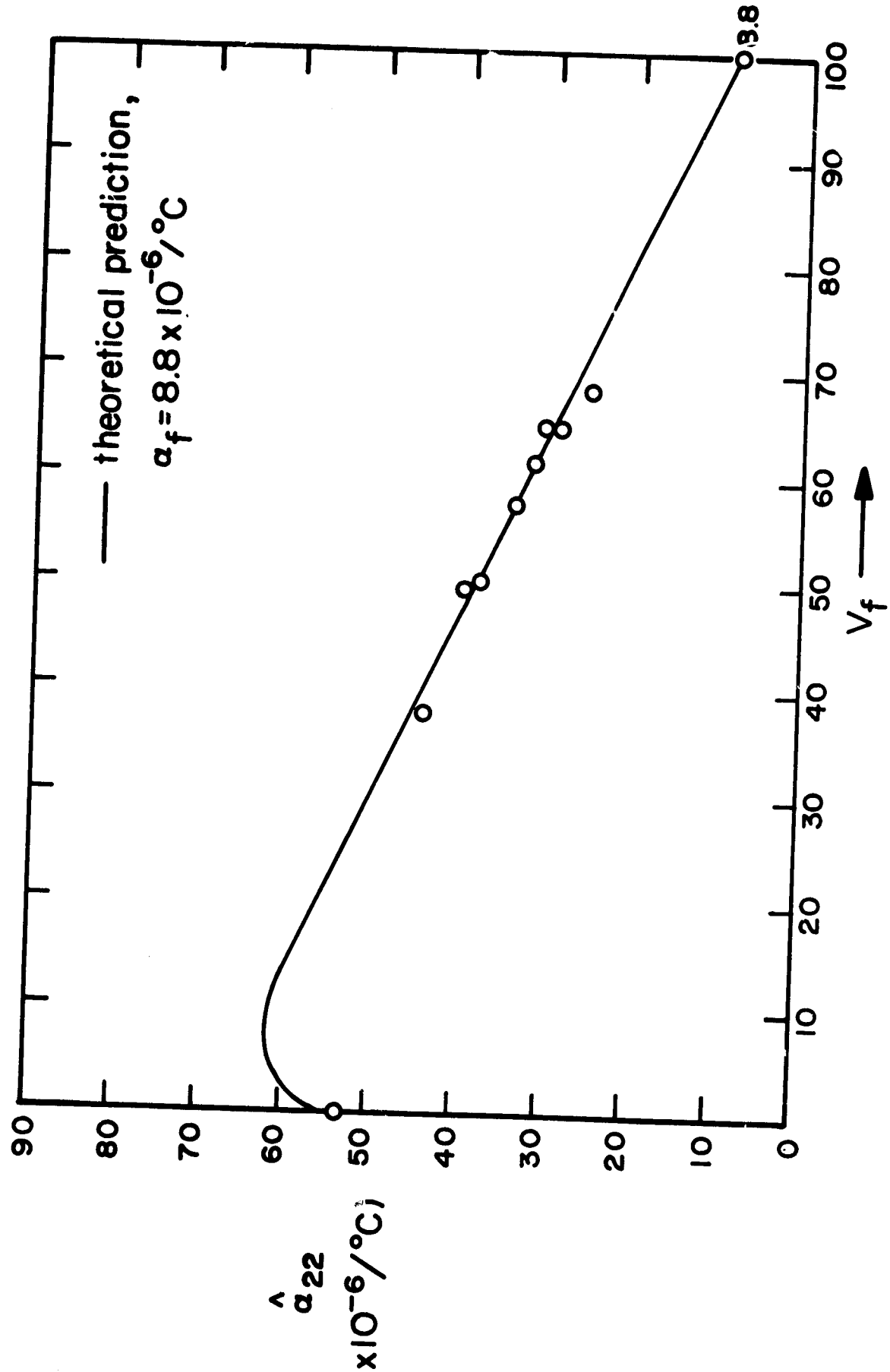

Figure 33

TCE versus Fiber Volume

at $V_f = 1$ is not satisfied. In order to satisfy this condition, the following must be true:

$$\lim_{V_f \to 1} \hat{\alpha}_{22} = (1 + \nu_{f_{12}})\alpha_{f_{22}} - \hat{\alpha}_a \nu_{f_{12}} \tag{11}$$

$$\text{as } V_f \to 1,\ \hat{\alpha}_{22} \to \alpha_{f_{22}} = \alpha_{f_{22}} + \nu_{f_{12}}\alpha_{f_{22}} - \hat{\alpha}_a \nu_{f_{12}} \tag{12}$$

$$\Rightarrow \hat{\alpha}_a = \alpha_{f_{22}} \tag{13}$$

The resulting equation is:

$$\hat{\alpha}_{22} = (1 - \nu_m)\alpha_m V_m + (V_f - \nu_m V_m)\alpha_{f_{22}} \tag{7b}$$

Input values used in the theoretical prediction plotted on Figure 33 are:

$$\nu_m = .35 \qquad \nu_{f_{12}} = .30 \text{ (Ref. 15)}$$

$$\alpha_m = 53.2 \times 10^{-6}/°C \qquad \alpha_{f_{22}} = 8.8 \times 10^{-6}/°C$$

$$E_m = .55 \times 10^6 \text{ psi} \qquad E_f = 32.5 \times 10^6 \text{ psi}$$

It is seen from Figure 33 that excellent correlation exists between experimental data and the results calculated from Equation (7b). The reason for the need to modify the form of the equation falls back on the hidden assumption in the derivation of Equation (7a) in the third term that the constituents are isotropic in nature. Equation (7a) assumes that $\hat{\alpha}_a \equiv \hat{\alpha}_{11}$ from isotropy and $\hat{\alpha}_a \simeq \frac{\overline{K\alpha}}{\overline{K}}$ where $\overline{K}$ is the volume ratio of the bulk modulus (i.e., $\Sigma K_n V_n$) and K is defined to be:

$$\frac{\sigma}{\varepsilon_{11} + \varepsilon_{22} + \varepsilon_{33} - \bar{\alpha}_v \bar{I}} \tag{14}$$

$\overline{K\alpha}$ is defined in the same manner. In Equation (14), $\hat{\alpha}_v$ is equal to $\hat{\alpha}_{11} + \hat{\alpha}_{22} + \hat{\alpha}_{33}$, which in the case of isotropic

C-2

constituents can be reduced to $\hat{\alpha}_v = 3\hat{\alpha}_{11}$. Substituting this isotropic constituent condition in Equation (14) and assuming that $\frac{\overline{E\alpha}}{\overline{E}} \simeq \frac{\overline{K\alpha}}{\overline{K}}$, Equation (7) is derived by energy principles.

References

1. Paul, B., "Prediction of Elastic Constants of Multiphase Materials", Transactions of the Metallurgical Society of AIME, Vol. 218, February 1960, p. 36.

2. Whitney, J. M. and M. B. Riley, "Elastic Properties of Fiber Reinforced Composite Materials", AIAA Journal, Vol. 4, No. 9, September 1966, p. 1537.

3. Hashin, Z. and W. B. Rosen, "The Elastic Moduli of Fiber Reinforced Materials", Transactions of the ASME, Journal of Applied Mechanics, June 1964, p. 223.

4. Chen, C. H. and S. Cheny, "Mechanical Properties of Fiber Reinforced Composite", Journal of Composite Materials, Vol. 1, 1967, p. 30.

5. Foye, R. L., "An Evaluation of Various Engineering Estimates of the Transverse Properties of Unidirectional Composites", SAMPE, Vol. 10, 1966, p. 631.

6. Greszczuk, L. B., "Thermoelastic Properties of Filamentary Composites", AIAA/ASME 6th Structures, Structural Dynamics and Material Conference, Palm Springs, California, 1965, p. 285.

7. Schapery, R. A., "Thermal Expansion Coefficients of Composite Materials Based on Energy Principles", Journal of Composite Materials, Vol. 2, July 1968, p. 380.

8. Chamis, C. C. and G. P. Sendeckyj, "Critique on Theories Predicting Thermoelastic Properties of Fibrous Composites", Journal of Composite Materials, Vol. 2, July 1968, p. 332.

9. Wang Fo-Fe, G. A., "Elastic Constants and Thermal Expansion of Certain Bodies with Inhomogeneous Regular Structure", Soviet Physics - Doklady, Vol. 11, No. 2, August 1966, p. 176.

10. Fahmy, A. H. and A. N. Ragai-Ellozy, "A Discrete Element Method for the Calculation of the Thermal Expansion Coefficients of Unidirectional Fiber Composites", paper presented at the 7th International Symposium on the Thermal Expansion of Solids, American Institute of Physics, Conference Proceedings No. 17, American Institute of Physics, 1973.

11. Kahn, K. H., "On the Thermal Expansion of Unidirectional Fiber Composites and Reinforcing Graphite Fibers", Doctoral Thesis, North Carolina State University at Raleigh, North Carolina, 1976.

12. Nakamura, H. H. and D. C. Larson, "Thermal Expansion Behavior of Boron/Epoxy and Graphite/Epoxy Advanced Composite Materials", paper presented at the 4th International Symposium on the Thermal Expansion of Solids, American Institute of Physics, Conference Proceedings No. 17, American Society of Physics, 1973.

13. Freeman, W. T. and M. D. Campbell, "Thermal Expansion Characteristics of Graphite Reinforced Composite Materials", Composite Materials: Testing and Design (Second Conference) ASTM STP 497, American Society for Testing and Materials, 1972, p. 121.

14. Kowalski, I. M., "Determination of the Elastic Properties of Orthotropic and Anisotropic Materials Using a Minimum Number of Tensile Tests", Master's Project, Rensselaer Polytechnic Institute, Troy, N. Y., May 1979.

15. Ishikawa, T., "Thermal Expansion Coefficients of Unidirectional Composites", Journal of Composite Materials, Vol. 12, April 1978, p. 153.

16. Tsai, S. W. and T. Hahn, Composite Materials Workbook, Technical Report AFML-TR-78-33, Air Force Materials Laboratory, Wright-Patterson Air Force Base, Ohio 45333.

17. Levin, V. M., "On the Coefficients of Thermal Expansion of Heterogeneous Materials", Mechanika Tuerdogo Tela (1967) p. 88.

18. Dean, G. D. and P. Turner, "The Elastic Properties of Carbon Fibres and Their Composites", Composites, July 1973, p. 174.

PART V

PERSONNEL

AUTHOR INDEX

PERSONNEL

Senior Investigators

Brunelle, E. J., Jr., Sc.D. (Aeroelastic and structures design and analysis, CAP-GLIDE)*	Associate Professor of Aeronautical Engineering
Das, P. K., Ph.D. (Non-destructive evaluation, research)*	Professor of Electrical and Systems Engineering
Diefendorf, R. J., Ph.D. (Fabrication, CAPGLIDE; fiber behavior, research)*	Professor of Materials Engineering
Feeser, L. J., Ph.D. (Computer applications and graphics, computer aided design, optimization)*	Professor of Civil Engineering
Hagerup, H. J., Ph.D. (Aerodynamics, configuration, pilot accommodation, CAPLGIDE)*	Associate Professor of Aeronautical Engineering
Helwig, G., Dr.Ing. (Finite element methods, computer aided design, composite structure optimization, CAPGLIDE)*	Research Assistant Professor of Aeronautical Engineering
Hoff, N. J. Ph.D. (Structural design and analysis, CAPGLIDE)*	John A. Clark and Edward T. Crossan Professor of Engineering
Krempl, E., Dr.Ing. (Fatigue studies, research)*	Professor of Mechanics and Director of Cyclic Strain Laboratory
Shephard, M., Ph.D. (Computer graphics, finite element methods)*	Assistant Professor of Civil Engineering
Sternstein, S. S., Ph.D. (Failure analysis, matrix behavior, research)*	William Weightman Walker Professor of Polymer Engineering

*Fields of Speciality

Stoloff, N. S., Ph.D. (Directionally solidified eutectics, research)*	Professor of Materials Engineering
Tiersten, H. F., Ph.D. (Non-destructive evaluation theory, research)*	Professor of Mechanics

Contributing Faculty

Kudva, N., Ph.D. (Post-buckling behavior)*	Assistant Professor of Aeronautical Engineering
McDonald, J. F., Ph.D. (NDE signal processing)*	Associate Professor of Electrical Engineering
Scarton, H., Ph.D. (Acoustic emission NDE)*	Associate Professor of Mechanical Engineering and Mechanics

Research Staff

Manager & Master Technician, Composites Laboratory

Haedelt, Volker

Research Associates

Kenmochi, Kiyoshi, Ph.D.
LeMaistre, Christopher, Ph.D.
Sinha, Bikash, K., Ph.D.

Graduate Assistants

Altman, Carl, B.A.
Berg, R. William, B.S.
Chen, Lien-Wen, M.S.
Esser, L., B.S.
Fisher, Mark Thomas, B.S.
Herbert, Paul, B.S.
Joshi, S., B.S.
Kim, Chul-Min, B.S.
Kim, Wonsub, B. S.
Lanzl, Colin. B.S.
Lumban Tobing, Frida, M.S.
Muser, Cristoph, Dipl.Mech.Ing.
Niu, Tyan-Min, M.S.
Shick, D. V., B.S.
Sundaram, Viswanath, M.S.
Taggart, David, B.S.
Uzoh, Cyprian, B.S.
Van Schoonveld, H. Garrit, B.S.
Yang, Phillip, B.S.

---

*Fields of Speciality

Undergraduate Assistants - Seniors*

Donnelly, J. Patrick
Ezzo, Jeffrey
Lenyo, John S.
Reusch, David
Rodgers, R. George
Shaefer, Paul
Shoales, Gregory A.
Venner, Joseph

Undergraduate Assistants - Juniors*

Borfitz, Michael
Chast, George
Coy, Paul F.
Dearborn, John
Emmel, John
Fallon, William
Flint, Fred
Fortune, James
Gorley, Ronald
Kearns, Thomas
Marchisotto, Paul
McGuire, Paul
Meyer, Edwin
Riker, Steven
Schriber, Steven
Schwitter, William
Snyder, Scott
Tavares, Mario
Witte, Mark

Undergraduate Assistants - Sophomores*

Grandin, Albert
Wetzel, Eric

*Status prior to Commencement and end of term in the Spring of 1979.

AUTHOR INDEX